Experimental Approach for Drug Profiling of Calcitriol in Yeast

By

Sasi Kumar Jagadeesan

Thesis submitted to the
Faculty of Graduate and Postdoctoral Studies
In partial fulfillment of the requirements for the degree
Master of Applied Science in Biomedical Engineering

Ottawa-Carleton Institute for Biomedical Engineering
School of Electrical Engineering and Computer Science
University of Ottawa
Ottawa, Ontario, Canada

uOttawa

Abstract

Vitamin D regulation is associated with several human disorders and contributes to various cellular mechanisms. Calcitriol (commercially available as Rocaltrol), an active Vitamin D metabolite, is known as a neuro-protective and anti-cancer drug but most importantly helps maintaining the calcium homeostasis inside the human body. The effectiveness of calcitriol to perform as an effective therapeutic agent is counteracted by its calcemic effects. In order to obtain better therapeutic results, synthetic calcitriol analogs without these calcemic effects have been recently developed but they are not yet cost-effective and their production is time-consuming. In order to determine the best active form of calcitriol that could provide higher chemotherapeutic activity without these calcemic effects, calcitriol mode of action was studied using yeast as a model system.

In order to achieve this, we analyzed the calcitriol effects on yeast cellular growth based on calcium intake levels. In this work, we also assessed yeast strains with gene deletions of selected calcium transporter genes to understand the calcitriol metabolism. For the aim of understanding hypercalcemic effects of calcitriol, we developed a hypothesis based on calcitriol interactions with oxygen. Interestingly, use of an anaerobic model validated the oxygen interactions with calcitriol that might possibly cause calcemic effects on patients. Anaerobically grown yeast treated with calcitriol showed significantly less intracellular calcium levels when imaged under indo-1 calcium binding fluorescence dye as compared to calcitriol treated yeast grown under aerobic conditions. Finally, we predict that calcitriol might control free radical generation within the yeast system based on experiments with AAPH and UV- irradiation.

Acknowledgements

I dedicate this thesis to my supervisors Dr. Mustapha C.E. Yagoub and Dr. Myron Smith. Without their guidance, encouragements and support, this research would not be possible.

Initially, I want to thank Dr. Yagoub for all his support in mentoring me towards this interesting research topic and for the guidance that he provided during the course of this study. I am deeply grateful to Dr. Myron Smith for his gracious support in welcoming to his laboratory and providing me with all the resources that helped me towards the successful completion of this project. I truly thank him for all his support and he will always remain as an inspiration to me throughout my life.

I am thankful to all my course instructors who have made my academic learning interesting and the uOttawa staff members who have helped my way to complete this thesis.

Finally, I want to thank my mom Mrs.Kumari Jagadeesan and my dad Mr. Jagadeesan Kathavarayan for all the love and support that they provided throughout my life.

Last but not least, my sincere thanks to my brother-in law Mr. UdayaKumar and my sister Mrs. Amudha Udayakumar for their guidance in pursuing my career.

Thanks to God!

Table of Contents

List of Figures

List of Tables

List of Abbreviations

1, 25OH_2D_3	1, 25-dihydroxyvitamin D3
25 (OH)D	25-hydroxycholecalciferol
AAPH	2, 2'-Azobis (2-amidinopropane) dihydrochloride
BLAST	Basic Local Alignment Search Tool
DHC	Dehydrocholesterol
F20T12/BLB	Fluorescent Black-light Blue Medium Bi-Pin Base
iGEMDOCK	Graphical Environment for Recognizing Pharmacological Interactions and Virtual Screening
IL	Interleukin
Kda	Kilodalton
Mcg	microgram
MIC	Minimum Inhibitory Concentration
NGF	Necrosis Growth Factor
nmole	nanomole
OD	Optical Density
PTH	Parathyroid Hormone
ROS	Reactive Oxygen Species
RXR	Retinoid X receptor
TSH	Thyroid Stimulating Hormone
VDD	Vitamin D Deficiency
VDR	Vitamin D Receptor
YPD	Yeast Peptone Dextrose

Chapter1. Introduction

Over the years, vitamin D (VD) has been capturing worldwide interest due to its diverse roles in regulating the body's metabolism and in preventing various chronic diseases including tumor progression. There has been a rising acclaim on the needs of Vitamin D and its deficiency associated effects in patients [1, 2]. Several factors such as indoor living, skin pigmentation, latitude/longitude regional location, climatic conditions, ozone depletion and personal sunlight exposure behaviors have contributed to increasing Vitamin D deficiency rate over the years [3]. It is notable that 90 % of overall vitamin D is synthesized from sunlight and only 10 % is from dietary supplements [4]. This need has encouraged researchers to understand the mechanism of Vitamin D and its vast roles in activities of the human body. Recent research studies have showed potential remediating Vitamin D mechanisms in overcoming numerous physiological disorders that mainly include diabetes mellitus, stroke, autoimmune diseases, coronary heart diseases and certain types of cancer [2, 5-7]. Interestingly, studies show that a particular vitamin D metabolite called calcitriol performs as an effective chemotherapeutic drug with other benefits, but its usage is limited due to its hypercalcemic effects on treated patients [8].

In this thesis, we planned to investigate the calcitriol mode of action using *in silico* modelling of yeast cells supported with experimental live cell-based data. In this procedure, we utilize bioinformatics as a platform for developing a yeast-based model system to examine the actions of calcitriol and its associated calcemic effects on treated human patients. Previous studies emphasize yeast cells as an effective modelling organism for drug developmental research, as it contains 60 % of the human gene homologs [9]. Yeast modelling is a more convenient and cost effective approach to conduct drug compartment modelling experiments. In this research, we modelled calcitriol based on yeast cellular calcium intake levels, oxidative stress analysis, free radical generation (ROS) and its anti-aging affects with an experimentally developed computational platform.

1.1 Vitamin D Metabolites

Vitamin D metabolites are generally produced from a photolytic process occurring over the cutaneous portion of skin. The photolytic process is defined by the exposure of sunlight at a UV-B band wavelength range of 292-300 nm, which is the corresponding wavelengths that stimulate the production of Vitamin D inside the body. This reaction occurs through a cholesterol derivative present in the skin called as 7-Dehydrocholesterol (7DHC) [10]. The developed vitamin D metabolites are used in different drug composition e.g. Carbamazepine and Valproic acid. These drugs stimulate the body's mechanism against several diseases. However, the role of Vitamin D metabolites in these protective mechanisms is yet to be determined [6]. These positive mechanisms of Vitamin D metabolites in human body suggests that we can employ an active vitamin D metabolite, calcitriol, to study its physiological role which might ideally serve as a proper enrichment source to develop effective Vitamin D drugs in the future. Recent studies have also indicated beneficial effects of calcitriol, however, the characteristic feature of calcitriol to perform as an effective therapeutic agent is counteracted by its calcemic effects [11]. Functionally, the treatment of calcitriol for various therapeutic purposes can be structurally manipulated in clinical applications by developing synthetic Vitamin D drugs which are minimally devoid of these calcemic effects. Pharmaceutical Engineering is indeed one of the most recently developed engineering disciplines – it sets out to modify naturally occurring drug formulations to provide effective treatments for various disorders. Although synthetic Vitamin D drugs have been delivering promise in anti-calcemic therapy, they are still not cost-effective and require a longer time during for production. Overall, it is still hard to obtain a useful synthetic Vitamin D drug for clinical applications without the calcemic effects [12, 13]. In this work, we used calcitriol, an active vitamin D metabolite produced in the kidneys, to understand the calcemic effects occurring at the cellular level.

Calcitriol as a drug regulates a vast majority of the body's calcium metabolism by increasing the intestinal calcium absorption. The malfunctioning of this hormone leads to hypercalcemic effects that cause chronic renal failure and cancer progression in patients [14]. Currently, this drug is prescribed only for hypocalcemia patients, but it could be broadly localized to target various parts of the tissue without imposing serious calcium threats to the treated patients [8]. For this purpose, understanding the calcium signaling effects of calcitriol is a basic step to developing an effective drug design for our proposed objective.

Drug designing initiates with a better understanding of drug analysis. The process of drug analysis follows the below-mentioned strategies: Computer Aided-Drug Designing, Receptor-Ligand targeting approach and by using animal models. The initial approach of drug analysis is conducted by a selective approach in developing a simple unicellular model organism that could be found compatible with humans. With this approach, the calcitriol function can be studied based on its various hypothesis and claims resourced from the literature on experimental basis accompanied by a systemically developed model. We, therefore, applied the concept of studying the mechanism of Calcitriol by using yeast as a model organism and thereby conjugating its effects in calcium homeostasis.

1.2 Problem Statement

Vitamin D metabolites developed synthetically with minimal calcemic effects provide a 3-150 times more effective cure rate than that of calcitriol in its natural form. However, the selection of the type of calcitriol analog to produce such selective responses has always been a complicated study in determining end effects [15]. Moreover, the production of these synthetic analogs is limited due to time constraints and high-cost. In addition to that, synthetic analogs have a complicated drug signaling mechanism compared with that of the natural form which might present a serious threat to the body in bringing other forms of life threatening diseases/disorders.

The important goal of this research is to assess the performance of a naturally available drug in the cellular mechanisms by inducing various calcium stress levels, thereby monitoring its biological activity based on its calcium interaction mechanisms. For this purpose, we investigated the use of yeast as a model organism in our drug analysis. Yeast is one of the ideal organisms that facilitate a detailed study on systems biology to elucidate the physiological and genomic properties of living cells. Yeast has become the pioneer organism over the last decades for conducting drug studies relevant to human. Calcitriol has the capacity to target individual cells [16]. Yeast cells might serve as an ideal model for understanding the responses of drug that include cellular metabolic activities such as cell-cell association, signal transduction, and transport of ions and nutrients. However, the problems of using calcitriol in research analysis are mainly related to the level of calcium toxicity one can be administered and the cost oriented with its synthetic version. The impact of calcitriol-mediated biological effects in the body systems is displayed in table 1.

Table 1 Effects of Calcitriol over various body target sites

Body systems	Target site	Biological Effects
Immune system	Macrophages, lymphocytes	Interferon and IL1 Suppression via IL6
Central nervous system	Ganglia, glial cells and hippocampus	NGF production, leukemia inhibiting factor
Epithelium/cancer	Keratinocyte, mammary, prostrate, colon, lung, female reproductive tract	Differentiation and cell growth arrest
Endocrine system	Thyroid, Pancreatic beta cell and ovary	TSH reduction and folliculogenesis with decreased cell proliferation
Muscle	Heart	Atrial Natriuretic Peptide reduced expression

From table 1, we can understand the active role of calcitriol in important compartments of the human body. The other major problems attributed to Vitamin D studies are minimal exposure of the human body to sunlight in recent years for various reasons added with enhanced ozone depletion have led to numerous Vitamin D deficiency related disorders [17]. Therefore, there is an increasing demand to model the signaling pathways of calcitriol by understanding its complex series of mechanisms inside the cellular activities. To achieve this purpose, the first step was to investigate the role of calcitriol with that of reliable data. Since there is a limitation in obtaining clinical data, the generic ideas from documented sources have served as a reference to build our model. This model employs a combinational approach of clinical microbiology and bioinformatics using yeast to develop a convincing reasoning for calcium effects inside the patients mediated by calcitriol. Once completed, we proposed a new model for an advanced developed configuration model which is based on a hypothesis developed from the resulting data of the experiments. Then, we made a comparative study to evaluate the hypothesis and to study its behavior based on its anti-aging and antioxidant properties. The resulting data from the overall research provides a detailed understanding of the signaling pathways of the molecule embedded inside the cytosolic and nuclear activities of the yeast cellular system.

1.3 Proposed Solutions and Contributions

The main reason for this work was to increase the usage of Vitamin D-like drugs for various purposes by decreasing toxicity and also the cost associated in producing its synthetic version.

The general achievement of understanding the drug pharmacokinetic system includes the following steps:

- Computer docking simulations for understanding protein interactions in a yeast environment.
- Creating systematic calcium stress inside the live cells using synthetic media.
- Performing a computer-aided approach for genomic analysis by selecting specific gene deletion mutants (abnormal cells) from gene deletion library.
- Detecting the cytosolic calcium concentration using fluorescence imaging technique.
- Understanding the protective mechanisms of calcitriol towards the reactive oxygen species (ROS) generation via 2, 2'-Azobis (2-amidinopropane) di hydrochloride (AAPH) and UVB irradiation exposure set up. Identifying calcitriol anti-aging and anti-tumor activities via chronological life span media.
- Experimenting with the oxygen affinity of the drug on various oxidative stress levels in an anaerobic chamber to determine its high binding capacity with the oxygen molecule that could cause hypercalcemic effects in treated patients.

1.4 Document Overview

The overall thesis consists of six chapters. Chapter 2 features background information on various topics related to the research and also the theory behind our proposed research which serves as a platform for our research. Chapter 3 explains the state of the art relevant to the roles of calcitriol in cellular activities. It depicts the calcitriol operative mechanisms in the yeast system and briefs the theories in using yeast as a model organisms for pharmacokinetic study. Chapter 4 deals with the experimental design for setting up the optimum parameters under various calcium stress levels. The first stage was setup based on developing optimum parameters for providing ideal conditions for the most suitable effect of calcitriol in the yeast system model. The second stage was indeed our main contribution. It investigated calcitriol operative mechanisms in an aerobic/anaerobic chamber to study the calcitriol-mediated calcemic effects in treated patients. Chapter 5 shows the obtained results for each model as well as it provides a comparative study by differentiating control vs calcitriol-treated cells. Finally, Chapter 6 concluded our research work and potentially summarizes some of its directions that can be explored as future work to further improve our understanding.

Chapter 2. Background and Literature Review

2.1 Vitamin D and its biological significance

Vitamin D is termed as “the sunshine vitamin”. Vitamin D metabolites are generally activated by Vitamin D receptors [18]. In humans, calcitriol is considered to be the most active form of Vitamin D. The calcitriol secretion is regulated by the production of parathyroid hormone (PTH) inside the body [19]. Almost half of the world population suffers from Vitamin D deficiency and the main symptom is hypocalcaemia [20]. The importance of vitamin D deficiency is revealed in certain revolutionary theories such as DINOMIT model developed by Garland Brothers which claims that the decrease in Vitamin D content increases the risk of cancer progression [21].

UV-B irradiation and vitamin D drugs are most commonly used therapies to overcome Vitamin D deficiency. However, irradiating live cell therapy is limited due to its associated risk of causing side effects to the healthy cells around the treated region. In a way, it is essential to secure the living frameworks away from these harmful effects of UV-B radiation, which is critical in the pharmaceutical study and in radiation science [22, 23]. It is likewise paramount in utilizing the other forms of Vitamin D such as vitamin D drugs to treat Vitamin D deficiency (VDD). However, these drugs have to be distributed based on a very high certainty of planning in order to provide a best therapeutic effect in each drug-fraction. For this, a general understanding of the calcitriol signaling mechanisms is necessary to understand its pattern of regulation in the human body. Vitamin D levels in the human body are generally defined by 25(OH) D content in the serum blood. Severe deficiency ranges at 12.5 nmol/L, the normal deficiency at 37.5 nmol/l, standard at 37.5-250 nmol/L and excess/intoxication level ranges at 275 nmol/L or above [24].

2.2 Calcium Homeostasis

Vitamin D is a major site of calcium interaction in humans. Calcium is a key element and regulates various roles in the body system. It is synthesized in three major organs that include intestine which serves as a site for calcium absorption, kidneys that provide a platform for calcium secretion and skeletal system that enhances bone mineralization. Figure 1 explains the Vitamin D-mediated calcium regulation in these three organs.

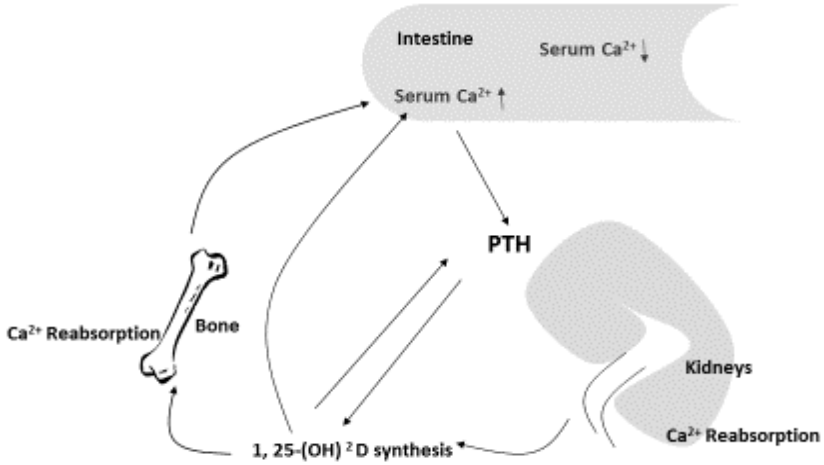

Figure 1 Calcium Homeostasis in Human Body

The diagram illustrates the VD (1, 25 OH^2D) mediated Ca^{2+} regulation occurring in kidneys, bone and intestine

2.3 Biological Calcification

Excess presence of calcium inside a tissue/cell/organ leads to biological calcification. Similarly, occupancy of inorganic substances along with a large amount of calcium phosphate and carbonate leads to the formation of calcified tissues. This process of calcification enables cells to build their hardness and quality. However, this excess calcium intake leads to calcium poisoning that could cause serious threats to the body. Several methods are used in determining this biological calcification, which mainly involves biophysical and biochemical methods. Here, we are about to discuss some of the techniques that contribute to calcification studies in the biological system.

2.3.1 X-Ray Diffraction

X-ray diffraction is the most widely utilized technique in identifying the material properties. It works on the principle that when a single beam of monochromatic x-ray radiation passes through a crystalline material, the beam scatters and the patterns are formed on a photographic plate. The distributed pattern follows the symmetry of the crystal. By measuring incident and scattered beams, we can identify the displacement between the reticular planes and the parameters of the crystal geometrical cell. According to Matsushima et al. [25], this method has a major disadvantage in identifying calcified tissues due to its weak degree of localization.

2.3.2 Neutron Diffraction

This method can overcome the defect produced in x-ray diffraction. It helps in differentiating the calcified tissues from that of non-calcified tissues by implementing the inelastic neutron scattering technique [26]. However, it implies high energy nuclear reactions to excite the neutrons, providing a high signal-noise ratio (1Mev equivalent of energy is released during this reaction) that could encompass improper quantification of calcified samples.

2.3.3 NMR spectroscopy

It is a unique method that allows positioning of a biological solution under high magnetic field and focuses the alignment of hydrogen spin controlled by electromagnetic radiation. Variance between the excited and normal alignment of hydrogen spin provides a spectrum that determines the structure of the analyzed sample. Fernandez-Seara et al. first studied this NMR detection for bone mineralization [27]. The accuracy of this method mainly depends on the purity of the compound and are limited to handle only liquid samples.

2.3.4 Electron Spin Resonance

It is an expensive approach as it requires paramagnetic particles stored below 20° K temperature. For detecting calcium mineralization in the solid sample, ionizing radiation such as Cobalt-60 (Co^{60}) delivers the irradiation of samples, which in turn determines the defects and allows differentiating the defect from another original compounds. This difference provides the calcium content in the crystalline sample [28]. ESR is welcomed for its high specificity, but it is dependent on free electrons and temperature.

2.3.5 Fluorescent Technique

Fluorescence technique is a more convenient approach in detecting calcification of cells using calcium-imaging dyes [29]. Fluorescence allows the analyzed molecule to emit the absorbed electromagnetic radiation / light to determine the structure composition. The principle behind this technique is defined by Beer-Lambert law [30].

$$F(\lambda_x, \lambda_m) = I_A \phi(\lambda_m) Z = [2.303 I_0 \varepsilon(\lambda_x) CL] \phi(\lambda_m) Z \quad (1)$$

Z is the instrumental factor, I_0 is the incident light intensity, Ɛ is the molar extinction coefficient, ϕ represents the quantum yield, C is the concentration, and L denotes the path length. This process is termed as fluorescence imaging as described in figure 2.

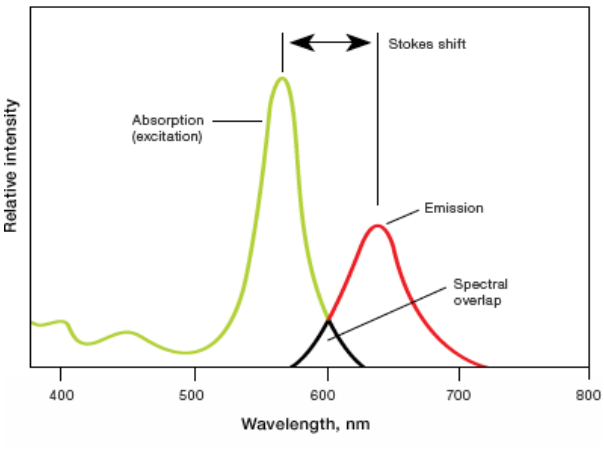

Figure 2 Fluorescent Intensity Detection [31].

The figure depicts the excitation and emission spectra of a fluorescence dye at different wavelengths

In figure 2, the emission spectrum depicts the lower energy and excitation spectrum displays a higher order emission due to electromagnetic radiation. The difference between the two is measured via stoke shift which denotes the absorption of same transition photon by the source that takes it to the excited state and emission state.

The above-discussed biophysical techniques face major difficulties because of limited availability and high cost in nature. In addition, the precision of the results obtained from these experiments may be low, leading to a minimal understanding of the calcification process. These techniques also undergo problems because of their weak targeting of the specimens and reduced localization effects. Most of the results obtained so far to get a better understanding of the calcified tissues are determined from biochemical methods. To overcome the disadvantages faced in these methods, we developed a cost-effective approach in detecting the calcified cells/tissues.

In order to achieve this motive, we finalized a study based on a biophysical technique, which utilizes a fluorescent light intensity detection method combined with that of a biochemical agent to illuminate the fluorescence levels. We implemented a simplistic approach by using a Fluorescent Detecting Plate Reader that could encompass the excitation and emission spectra of the biochemical agent that we are going to use in our research. The biochemical agent that we targeted is Indo-1 Penta-potassium dye. This dye fluoresces at emission spectra of 410 nm wavelength and excites at 480nm wavelength [32].

2.3 Biological Properties of Vitamin D

Apart from calcemic effects, certain other important phenomenon revolves around Vitamin D functioning and its production. The primitive source of Vitamin D synthesis develops from sunlight exposure. The exposure of direct sunlight over the skin site can make irreversible and detrimental changes in the cells because natural sunlight comprises Ultraviolet A, B, C, Visible light and infrared radiation A, B and C. In contrast to that, UV-B irradiation is also defined as the only defined carcinogen to have positive health benefits on humans [33-37]. Along with UV-B irradiation, other Vitamin D metabolites used in the treatment of vitamin D deficiency are calcifediol, cholecalciferol and calcitriol. Even though calcitriol and calcifediol pharmacokinetic activity appear to be comparable, the half-life for calcifediol is vastly reduced when compared with that of calcitriol which is mainly regulated by PTH [38, 39].

Calcitriol is defined as white, crystalline, organic molecule with a molecular formula (Mf) = $C_{27}H_{44}O_3$ and molecular weight (MW) = 416.63646 g/mol. The chemical structure of Calcitriol (PubChem CID: 5280453) is (1R, 3S, 5Z)-5-[(2E)-2-[(1R, 3aS, 7aR)-1-[(2R)-6-hydroxy-6-methylheptan-2-yl]-7a-methyl-2, 3, 3a, 5, 6, 7-hexahydro-1H-inden-4-ylidene] ethylidene]-4-methylidenecyclohexane-1, 3-diol and its structure is depicted in figure 3.

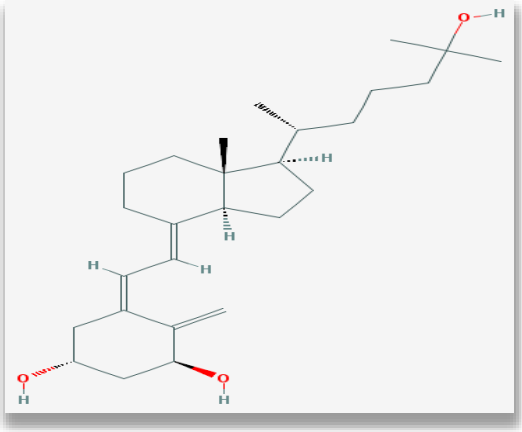

Figure 3 Chemical Structure of Calcitriol [40]

2.4 Pharmacokinetics

It is important to understand the pharmacokinetics of calcitriol inside the human system to develop our yeast model. Pharmacokinetics is a dedicated branch of science to study a molecule based on its therapeutic performance. It primarily focuses on drug analysis via the following steps: Absorption, Distribution, Metabolism and Excretion “Elimination” (ADME).

2.4.1 Pharmacological Dimension of Calcitriol

As discussed earlier, two calcitriol treatments are readily available: as a drug and as a radiation therapy. Calcitriol via drug form reduces the likelihood of prolonged and acute radiobiological effects from harmful UV radiations at the skin site [41]. It helps to recover the ATP utilization, during the cycle of its production via sunlight source.

2.4.2 Calcitriol Pharmacokinetics

Calcitriol is a common physiological hormone that the body synthesizes regularly from 0.5 to 1.0 mcg per day [42]. Uremic patients synthesize less calcitriol resulting in metabolic bone disease and chronic renal failure. Calcitriol is a powerful counteractive to these conditions which can stimulate the intestinal calcium absorption and maintains calcium homeostasis. The maximal serum calcitriol concentrations happen within 3-6 hours of drug administration and the elimination occurs following 5-8 hours via urine and feces for every single dosage of 0.25 mcg, 0.5mcg, and 1 mcg individually [43]. The dose description is provided in table 2. The starting phase of calcitriol pharmacokinetics is the retention/absorption stage that happens after medication consumption orally with 0.25 mcg or 1 mcg. Because of its minimal consistency and efficiency connected with the intake of the drug, it prompts intense calcemic effects in the blood serum compared to other types of calcium medications administered in the body.

Table 2 Calcitriol Pharmacokinetics data based on reference **[43]**.

Pharmacokinetic Time line	**Calcitriol Bioavailability in Serum pg/ml**
2 hours (Peak)	40.0 ± 4.4 to 60.0 ± 4.4
4 hours	53.0 ± 6.9
8 hours	50.0 ± 7.0
12 hours	44.0 ± 4.6
24 hours	41.5 ± 5.1

The second stage is the bio-distribution of calcitriol inside the human body. The highest site of calcitriol action occurs in the intestine and it is bound to 99.9 % in serum plasma.

The third phase of the pharmacokinetic study is the drug metabolism. It forms a Vitamin D complex with Vitamin D response element, retinoid x-receptor, vitamin D receptor (VDR) and other co-factors initiating the RNA transcription on the target gene. Calcitriol in its drug form can be metabolized via two pathways, the former is due to hydroxylation of the compound yielding calcitroic acid in the kidneys and the latter follows the formation of lactone products.

In the elimination stage, calcitriol is excreted via urine or feces from the plasma with a half-life of 5-8 hours [43]. Calcitriol has a much faster clearance when compared to other drugs. Calcitriol, in general, performs agonistic and antagonistic actions on human metabolism, which are yet to be investigated.

2.5 State of the Art

Several drugs used in the treatment of neurological conditions such as epilepsy induce vitamin D synthesis inside the body [44]. This shows the importance of vitamin D regulation occurring over various metabolic activities. However, the calcemic effects produced from the treated vitamin D drugs inhibit their therapeutic performance. To address this situation, advances in research have contributed to the production of Vitamin D synthetic analogs in order to obtain anti-calcemic activity [45]. These analogues help improve the target specificity of the drug by excluding its waste of energy in unwanted processes. However until now, none of these analogs are non-calcemic completely in the clinical setting and the cost associated with the production of these analogs is seemingly high [46]. To overcome these problems, we tried to contribute to the overall research by understanding the course of calcitriol actions in causing these calcemic effects with that of a yeast model. Insights on calcium metabolism in cell survival including calcium intake levels and calcium toxicity to calcitriol will provide a clear view in understanding the importance of sunshine vitamin active drug, calcitriol.

2.6 Conclusion

In this chapter, we exposed the biological phenomena of calcitriol and explained biological properties. The next study will be to setup our yeast model based on mathematical derivations, computational platform and the hypothesis that we developed to understand its functions inside the cellular model. Therefore, chapter 3 will be devoted to the yeast modelling theory based on calcitriol-mediated signaling mechanisms.

Chapter 3. Yeast Model Theory for Calcitriol Mediated Calcium Signaling Networks

3.1 Yeast as a human model

At a glance, it will not be convincing to compare baker's yeast with the complicated human model. Yeast has its own impediments and we cannot entirely rely on the results produced from this model. In general, the human body is composed of complex cellular mechanisms and yeast cannot reproduce this complete system in its biological activities. However, contrasting to these dimensions, yeast cells contain homologs of almost 65% of human genes and, significantly, share 25% of the human disease-related genes [9]. This makes yeast a considerable model framework for better understanding of complex cellular mechanisms in humans. Yeast also has advantages to other models in molecular biology due to its rapid growth that exhibits a doubling time of 1.5-3 hours allowing faster scale-up [47]. Another advantage of using yeast model is the availability of gene deletion library which facilitates identifying the role of genes associated with a particular function of that specific compound. These benefits permit yeast to be used as an efficient model in understanding the signaling pathways of calcitriol. In this chapter, we will be using yeast as our developmental model grouped under four stages which involve computational designing, experimental analysis, hypothesis development and finally evaluating the hypothesis based on the validation of obtained data.

3.2 Theoretical Background of Yeast modelled calcium transportation: First Model

The theoretical background of yeast calcium transportation in comparison with humans can be developed via two ways

1. Mathematical modelling of calcium transportation
2. Bioinformatics tools

3.2.1 Mathematical modelling of calcium homeostasis in yeast.

The transportation of calcium in yeast is regulated via several calcium channels, pumps and calcium binding proteins, which are commonly grouped together as “Molecular Toolkit” for calcium signaling networks.

Cytosolic free calcium plays a crucial role in cell stability which marks its standard for its high complexity relating to the understanding of its mechanism. A certain degree of dysregulation occurring in the cytosolic calcium levels could lead to various medical conditions including the cancer in humans.

In yeast, normal cytosolic calcium levels are regulated in a range of 50-200 nM with a typical atmospheric setting where calcium levels vary from <1 µM to > 100 mM [48]. Calcium transportation in yeast model initiates with the entry of extracellular calcium ions into the cytosol via transporter X. The ion transportation then takes different paths: (a) vacuolar calcium transportation, (b) cytosolic calcium transportation, and (c) cell organelles/nuclear calcium transportation. Vacuolar calcium transportation is facilitated by yeast calcium channels such as PMC1, VCX1 and YVC1. The cytosolic calcium transportation is backed up with two unknown proteins, transporter X and transporter M which mediate the calcium entry into the cell via cytosol. Certain other calcium pumps including PMR1, CCH1, and MID1 facilitates the calcium transportation into the cell organelles including the nucleus [49].

The equations described in [49] provides the mathematical modelling of yeast calcium transport via cytosolic, vacuolar and cell organelles (Golgi-apparatus, endoplasmic reticulum). The derivation for cytosolic calcium modelling is provided by,

$$\frac{\Delta\,[Ca_{ex}]}{[Ca_{ex}]} < \frac{{}_0\int^{2.5h} U(t)dt \times (2.5\times 10^7\ cells/ml)}{[Ca_{ex}] \times 100\ \%} < 5\ \% \quad (2)$$

where [ ] refers to concentration, $[Ca_{ex}]$ represents the cytosolic Ca^{2+} ion concentration and U (t) the X-transporter transfer rate of calcium ions from extracellular calcium concentration.

This equation describes the cytosolic calcium transportation and supports the theory that extracellular calcium ions favorably induce changes in the calcium homeostasis. The 5 x 10^7 cells/ml depicts the normal range of yeast cell numbers during normal growth under optimal conditions.

The governing equation for vacuolar calcium transportation is given as [49],

$$\Delta\,[\mathrm{Ca}_{\text{vacuole}}] \;<\; \frac{{}_0\!\int^{t} U(y)\,dy}{(33.5\,e^{\alpha t}\,\mu m^3 \times 50\,\%)} \;<\; 32mM \qquad (3)$$

The final equation contributing to assumption made that [Ca $_{ex}$] is constant and vacuolar calcium concentration is reduced to 10 % due to saturation of ions during cell growth is [49]

$$\Delta\,[\mathrm{Ca}_{\text{ER \& Golgi}}] \;<\; \frac{{}_0\!\int^{t} U(y)\,dy \times 10\,\%}{(33.5\,e^{\alpha t}\,\mu m^3 \times 10\,\%)} \;<\; 16mM \qquad (4)$$

The equation serves as a mathematical model for calcium homeostasis in yeast. This understanding paves the pathway for a computational approach using bioinformatics tools for a comparative study on calcium homeostasis in yeast cells and Vitamin D-mediated calcium signaling networks.

3.2.2 Bioinformatic Modelling (Receptor – Ligand interaction)

The movement of proteins and biological compounds around the body is circulated via blood and correspondingly it is targeted to a specific receptor into the cell through an active process called receptor-ligand interaction. The ligand is a biological molecule that binds to the active site of the target protein (receptor). This binding interaction of ligand-receptor results in the activation of the protein. This activated protein could perform various cellular functions including changes in the ionic channels, electrical transport inside the cell and cell differentiation. The above reaction for drug binding to the respective receptor is given by the law of mass action [50],

$$L\ (\text{Ligand}) + R\ (\text{Receptor}) \leftrightarrow L.R \qquad (5)$$

In our study, we choose calcitriol as a ligand and predicted its binding affinity with main calcium receptors present in yeast in comparison with human VDR using a docking methodology.

3.3 Molecular Docking simulations

Docking simulations analyze the molecular interactions using strategies such as predicting the receptor binding site, followed by a virtual screening of the bound molecules. This helps to estimate the binding affinity of receptor-ligand interaction by free energy predictions. The simulations on a molecular docking environment mainly depend upon search strategy and free energy estimation in determining the least used energy model. Finally, we could identify the best binding model with less utilization of Adenosine Triphosphate (ATP), a form of intracellular energy molecule that is involved in all cellular functions. The first stage in molecular simulations is the search strategy that basically leads to developing a search algorithm to predict the necessary molecules for simulation analysis. The next stage is the actual docking using a docking software such as Auto dock 4.0 or iGEMDOCK [51]. Conclusively, docking techniques are governed by approximations/predictions that use a computational approach and do not fully mimic the biological interactions occurring in the native state. However, initial predictions obtained using this technique will provide insights for our future research to develop a predictive model before we enter into the experimental phase.

3.3.1 Search Strategy

The molecular docking procedure initiates with search strategies for ligand adaptations by a scoring method. The most important goal of the search strategies is to foresee the binding affinities of the molecule and to assess the strength of the binding interaction.

For this purpose, we used a Protein Database (PDB) tool to identify the target protein molecules that are of main interest for our research. Research Collaborator for Structural Bioinformatics (RCSB) is a 3D structural database that provides three-dimensional geometry of structural proteins for research purposes [52]. We used PDB identifiers to identify protein structures in an open source software called PYMOL [53]. For our research purpose, we employed these strategies to explore the structural compliance of the yeast compartments for the human build.

3.3.2 Scoring Function

The actual molecular docking process begins with this method where we input the ligand-receptor structures into a docking software and allow them to run by defining their coordinates. General Docking programs provide minimum compatibility starting from predicting molecular interactions to final post-docking analysis. The docking software that we employed for our research is iGEMDOCK. This software could overcome this defect by synchronizing pre- and post-virtual screening docking methods in a graphical interface. Moreover, the results acquired from this technique strongly coordinates with 78% of the original data obtained from experimental results, which is one added advantage of using this technique [54]. With the derived data, we could stretch forward the research from protein-calcitriol interactions to gene sequence similarity.

3.3.3 EMBOSS STRETCHER Tool

Gene sequence matches are conducted on a bioinformatics platform called European Molecular Biology Open Software Suite (EMBOSS), that adjusts to data in a blended pack of associations and grants clear recuperation of sequencing information from the worldwide connection. We implemented STRETCHER tool, which is an application from EMBOSS that enables the linear alignment of two individual sequences and provides a scoring function. This tool specifically identifies the global gene sequence match of two proteins, which substantially permits the use of calcitriol interaction with docked proteins [55]. From this analysis, we could predict the structural and genomic responses of certain identified calcium transporters in yeast to that of calcitriol.

3.4 Microbiological Modelling: Second Model

Following the docking simulations, we employ microbiological techniques to understand the calcitriol functioning on live yeast cells. For this specific purpose of our research, we followed the traditional microbiological techniques using a yeast microorganism: *Saccharomyces cerevisiae* (Budding yeast: S288C strain) which is considered as a human biological model in our studies.

3.4.1 Anti-microbial sensitivity test by minimum inhibitory concentration (MIC) analysis

Initially, we conducted MIC tests that is defined as the minimum inhibitory concentration of the drug needed to arrest the growth of the microorganism. MIC is set as a gold standard for analyzing the performance of a drug towards any infectious microorganisms. In our research, MIC was conducted using a dilution range of calcitriol to test its efficacy over microbial growth [56]. This will be further elaborated in the next chapter.

3.4.2 Calcium stress response levels

Calcium level transition triggers a variety of cellular processes in every species. Calcium levels are usually analyzed in yeast cells by inducing various stress factors such as alpha factor, glucose, sphingosine, alkalinity, and other stress conditions. Under normal cellular conditions, extracellular calcium levels are maintained almost constant while during abnormal conditions could elevate to a higher level [57]. We reproduced certain stress conditions in yeast growth environment by using a synthetic medium with various levels of calcium to analyze the effect of calcium intake levels with that of calcitriol/non-calcitriol. These conditions help elucidate the cytotoxicity levels of calcium in yeast in regards to calcitriol. Calcitriol is also primarily responsible for its protective effect to overcome the toxicity caused by other compounds inside the cell [58]. The final output of the research should help to determine the toxicity/survival rate produced by calcitriol under various calcium optimal settings.

3.5 Mutant Approach: Third Model

To understand the genomic regulation of calcitriol related mechanisms inside the yeast cellular system, certain mutants are screened and tested to detect the effect of calcitriol within them.

3.5.1 BLAST technique

Basic Local Alignment Search Tool (BLAST) is an important technique used to screen the list of mutants similar to the human genome. BLAST works on a dynamic programming algorithm to compare the alignment scoring of two individual proteins, nucleotide or an amino acid sequence. [60]. After screening the mutants using BLAST technique, we isolated and cultivated these mutants using a yeast gene deletion library array.

3.6 Calcemic Effects of Calcitriol: Fourth Model

To address the calcemic effects of calcitriol, we developed a hypothesis based on a literature study. Calcitriol is generally transported to different target sites in the human body via blood. There are two types of biological proteins that facilitate this transportation: Vitamin D Binding Proteins and Vitamin D-dependent Binding proteins. Vitamin D Binding proteins are primary proteins that bind with calcitriol and transport it to the target tissues, whereas Vitamin D-dependent binding proteins permit the efficient transport of Vitamin D binding proteins in reaching the target sites. Until now, the known Vitamin D binding proteins are Calbindin-9kda, 28kda, 29kda and S100 [61]. All of these proteins are similar in having EF binding sites within them that have a high affinity towards calcium ions.

3.6.1 EF-hand Binding motif

Calcium binding proteins in all organisms carry a structural binding motif called EF-motif. EF-motif is termed as helix-loop-helix motif which could accommodate calcium ions within their structure. The calcium binding region within them generally consists of six residues in which five residues are found to be aspartate and glutamate and these residues contain oxygen side chains. Aspartate and glutamate are negatively charged amino acids and are referred as bidentate ligands (i.e., electron donors). The most interesting phenomenon occurring in these five residues is the negative charge nature of these residues that attracts the positively charged calcium ions thereby neutralizing them. In addition to that, the sixth residue undergoes side chain conformation by forming Carboxylates RCOO- and carbonyl groups C=O. Both carboxylates and carbonyl groups are of negative charge in nature and also have an oxygen atom. The EF structure is present in all calcium effector proteins in living cells [61]. This provides a basic understanding that calcium ions (Ca^{2+}) that are positively charged in nature should have high affinity towards negatively charged oxygen ions (O^{2-}). Excess calcium ions steadily transported in cytosolic calcium concentration might have a high affinity towards oxygen due to its positive charge nature. Therefore, we are developing a working model based on the developed hypothesis.

3.6.2 Hypothesis

The main function of Vitamin D is to stimulate calcium sequestration and regulate calcium levels within the body, primarily for bone synthesis. In this work, we proposed a hypothesis based on the increasing serum calcium in the human body mediated by calcitriol that causes hypercalcemic conditions. We propose that excess calcitriol circulated in the blood by Vitamin D binding proteins might have an affinity towards oxygen elements present in the blood circulation that ultimately raise the serum calcium levels leading to hypercalcemia conditions in calcitriol-treated patients. Recent research studies further support this theory stating that Vitamin D might have an effect on the oxygen mediated process such as glucose metabolism [62]. To implement our developed hypothesis in our study, we developed an anaerobic model that might produce beneficial outcomes to understand the oxygen affinity of calcitriol.

3.6.3 Vitamin D as an Anti-oxidant: Oxidative stress Analysis

Our developed view behind the oxygen affinity of the drug can also be well explored by using oxidative stress analysis based on the previous research studies [63, 64]. This study will significantly test whether calcitriol has the potential to bind with free oxygen elements in blood circulation.

3.6.4 AAPH

To explore the oxygen affinity of the drug further in detail, we tested calcitriol-treated cells with toxic chemical agents. There are several free radical synthesizing compounds such as superoxide and oxybenzone that could produce reactive oxygen radicals. However, the most commonly used compound is hydrogen peroxide. The main disadvantage of using this compound for our research is due to its fluctuations of free radical generation [65]. In order to have a gradual production of free radicals, we utilized AAPH (2, 2′-Azobis (2-amidino propane) dihydrochloride) which is a hydrophilic free radical generating compound that induces radical production in the aqueous state with a half-life of 175 hour [66].

3.6.5 UV-A irradiated deduced free radicals

Another counteractive research was conducted based on UVA irradiation ranging from 360 nm to 420 nm which has been used as an oxidative stress causing agent [67].

The claimed results so far by previous researchers have pointed out the risk of using UVA based-tanning or -medical therapy equipment in the interest of public health [68]. It is agreed that UVA occupies 90 % of the sunlight reaching the atmosphere. For the risk associated with UVA and also to elucidate the antioxidant properties of calcitriol, we developed an irradiation exposure set up to irradiate the yeast cells treated with calcitriol to identify the antioxidant properties and also to identify the oxygen affinity of calcitriol causing these calcemic effects.

3.6.6 Yeast as an anti-aging model

There are two aging models generally developed using yeast. One is a replicative aging model and the other is chronological life span method [69]. Replicative aging is based on the cell division from mother to daughter cells and the chronological life span method is based on the cell survival in a non-replicating conditions which we implemented in our research.

3.7 Conclusion

In this work, we focused on four kinds of yeast models to perform a comparative study on improvement/pernicious cellular activities during calcitriol treatment. Every model is composed of a reference model¸ which is used as a control to study the effective parameters for calcitriol functions and its associated metabolic activities. The initial model was developed to investigate the receptor-ligand docking mechanism of calcitriol in yeast using iGEMDOCK. The obtained results from this model provide a gateway for identifying the binding interactions of calcitriol with cellular proteins, recommending the use of yeast as a human model. The second model is an experimental model developed based on drug profiling to determine the calcium intake levels in yeast cells and to identify the optimum concentration parameters for calcitriol. The third model incorporates two major techniques: Gene deletion library and BLAST technique (another bioinformatics tool) which was used to identify Vitamin D-interacting homologs in yeast. The final model employs an anaerobic experimental set up to understand the oxygen affinity of calcitriol. With the above understanding, we finalized our study based on three important hypotheses revolve around Vitamin D; one on its calcemic properties and the other on its therapeutic effects and, finally, by elucidating its antioxidant and anti-aging properties. Chapter 4 will provide the whole framework of these four models followed by the obtained results explained in Chapter 5.

Chapter 4 Experimental Procedure and Data Acquisition

4.1 Drug Modelling

To understand calcitriol interactions in yeast calcium signaling proteins, a class of receptors that support the transportation of calcium ions have been selected from the literature [48, 70]. The final screened proteins are listed in table 3. The protein structures are obtained from the Protein Databank (PDB ID: VDX) [52]. The gene sequence for the corresponding proteins is provided in the Universal Protein Resource[1] database.

Table 3 Docked Calcium Transporters in Yeast System [70]

The table lists the selected calcium-related yeast proteins for docking procedure

S. no	Protein (Receptors)	Function	PDB ID	Organism
1	Mid1	Ca^{2+} transporter, calcium permeable channel, facilitates ER stimulated ca^{2+} ions	4XOH	Saccharomyces cerevisiae
2	VCX1	Ca^{2+}/H^{+} exchanger, restores cytosolic and vacuolar calcium levels during ca^{2+} depletion	4K1C	Saccharomyces cerevisiae
3	CMD1	This gene in yeast shares 60% of human genome; renowned eukaryotic Ca^{2+} transporter	4DS7	Saccharomyces cerevisiae
4	SNF4	Vitamin D receptor homolog in yeast and also responsible glucose metabolism and calcium transport	2NYC	Saccharomyces cerevisiae
5	YVC1	Only human TRP homolog present in yeast responsible for vacuolar calcium transport	2PNN	Saccharomyces cerevisiae
6	TRPA1	Close resemblance with YVC1 in yeast; mediates Ca^{2+} influx	3J9P	Human Homo sapiens
7	VDR	Vitamin D receptor for Vitamin D metabolism in humans, responds to various calcium signaling proteins in humans	1DB1	Human Homo sapiens

4.2 Pharmacokinetic action of the drug in yeast system

For our experiments, we purchased 30 micrograms of calcitriol from the pharmacy (i.e., 60 capsules of 0.5 micrograms each). The purchased capsules were pierced using a sterilized needle and the liquid calcitriol was extracted from the shell of the capsule by centrifugation conducted at a speed of 8000 rpm (revolutions per minute) over a time period of 2 minutes.

4.2.1 Determining the physiological parameters

There are different physiological parameters for every organism. In human, the physiological parameters vary for each tissue and organ. The pharmacokinetic parameters for the drug described in the literature substantially suit for the human model. The optimal conditions for yeast growth provided in the literature are as follows [70],

Temperature	:	30°C
pH	:	5-5.5
Doubling time	:	1.25-2 hours
Normal Cytosolic Ca2+ level	:	50-200 nm

Such conditions for yeast growth were maintained during the course of our research. To determine the concentration profiling based on calcium toxicity/survival, we optimized the calcium concentration intake levels in yeast.

4.2.2 Volumes/Cell Density of the System

The concentration of the drug from the site of intake till reaching the target tissue must undergo standard order of transportation. To evaluate this phenomenon, we have to signify the number of cells that are to be used for calcitriol treatment. By using UV spectrophotometer, we quantified the number of cells by optical density measurement. One Optical Density at wavelength 600 nm is equivalent to approximately 3×10^7 yeast cells/ml. Saccharomyces cerevisiae (S288c) has been streaked and plated on a petri-dish agar plate and left over in the incubator (temperature 30°C) for 48 hours. The 48 hour time period is sufficient for the yeast colonies to grow over the surface of the streaked plate. The media composition used for the growth of yeast cells are summarized in Table 4.

Table 4 Yeast Media Composition

YPD Agar medium composition (%, Concentration)	YPD Broth Medium Composition (%, Concentration)
2% Yeast Extract	2% Yeast Extract
4% Bactopeptone	4% Bactopeptone
4% Dextrose	4% Dextrose
4% Agar	

The cell population has been maintained by several subcultures at a constant optimum temperature (30°C) placed in an incubator until the end of our experiment.

The required amount of cells is obtained based on the following calculation,

$$OD1 \times V1 = OD2 \times V2 \quad (8)$$

Where,

OD1 = Optical Density of the broth culture inoculated overnight
V1 = unknown volume to be found (ml)
OD2 = Required Optical Density needed for the inoculum
V2 = final volume (ml)

Optical Density provides a measure of cell count present in the solution determined from a spectrophotometer at a wavelength of 600nm. Every experiment was initiated with the autoclaving procedure, which is one type of sterilization process to avoid any unwanted contamination.

4.2.3 Concentration Profile

In order to reach the goal of understanding the calcium signaling effects of the drug, the drug was optimized with different cellular calcium concentration to develop a concentration profiling of yeast. The experimental setting for MIC analysis is described below.

Procedure:

1. The drug stock solution is prepared (calcitriol; 0.5 mcg) for a volume of 700 µl in 1 ml centrifuge tube and kept refrigerated. The initial drug concentration used was 0.50 µg/l, 0.25 µg/l, 0.125 µg/l, 0.062 µg/l, 0.031 µg/l and 0.015 µg/l.
2. The cells are obtained from OD measurement with cell culture. The cells numbers are calculated for a range of 1.5×10^7 cells/ml.
3. We then developed the dilution range mentioned in Table 5 with calcitriol as drug and water as a control in a 96 well plate.
4. The volume of each well throughout the procedure is maintained at 200 µl.
5. The starting well A1 contains 170 µl of YPD cell culture treated with 30 µl of stock calcitriol. This is further diluted on corresponding wells with varying concentrations.
6. A triplicate was created on the initial three rows followed by a triplicate with sterilized water which serves as a control.
7. The cell plate is incubated for 24h at a temperature of 30°C in an incubator with shaking.
8. The parameter settings are optimized and the sequence must be validated successfully to run the detection process in a plate reader.
9. The final readings are obtained.

Table 5 MIC Plate Setup

The table contains calcitriol concentrations of 0.50 µg/l, 0.25 µg/l, 0.125 µg/l, 0.062 µg/l, 0.031 µg/l and 0.015 µg/l and control as water (W). The whole procedure is conducted in triplicates.

	1	2	3	4	5	6	7	8	9	10	11	12
A	0.50µg/l	0.25µg/l	0.12µg/l	0.06µg/l	0.03µg/l	0.01µg/l						
B	0.50µg/l	0.25µg/l	0.12µg/l	0.06µg/l	0.03µg/l	0.01µg/l						
C	0.50µg/l	0.25µg/l	0.12µg/l	0.06µg/l	0.03µg/l	0.01µg/l						
D	W	W	W	W	W	W						
E	W	W	W	W	W	W						
F	W	W	W	W	W	W						
G												
H												

4.3 Cell physiological parameters

The cell physiological parameters indeed provide information regarding the calcitriol transportation inside the cellular channels. For the optimum calcium concentration analysis, we varied the concentration profile by differing calcium ion concentration range and keeping the other constituents constant. Finally, the optimal calcium concentration for calcitriol was identified from our analysis.

4.3.1 Experimental Setup for Drug Concentration Profiling.

The general calcium parameters for the yeast environment are identified from the reference cell sample. Calcitriol dose (0.5 mcg) was treated with yeast cells for a period of 24 hours.

Procedure:

1. Initially, the Ca^{2+} ion composition for yeast medium (YPD) is calculated.
2. Media preparation is done accordingly to induce calcium stress on cell growth under three various stages.
3. The first stage of cell-mediated calcium stress response is induced by preparing four different calcium concentration media. The media constituents are listed in Appendices section. The rationale of this research brings in a better understanding of the calcitriol related calcium triggering responses in the cellular environment. The plate set up for this study is listed in Table 6.
4. The second stage of calcium stress response analysis is based on standard set of Ca^{2+} concentration profiling which allows the measurement of Ca^{2+} concentration range responsible for cell survival and toxicity dose levels related to calcitriol. The concentration media is described in Appendices and plate set up in Table 7.
5. The third stage of calcium stress response analysis is assessed to achieve the final optimized calcium concentration for cell growth rate produced by the drug in yeast environment. This is referred as the ideal therapeutic calcium concentration (ITCC) for

calcitriol on yeast growth. The plate set up is explained in Table 8 and the concentration set up is described in Appendices. The determined optimum concentration serves as the yeast pharmacokinetic concentration parameter of calcitriol.

Table 6 Calcitriol conditions: Stage 1 Plate set up

The table highlights normal (blue), deficient (green), and excess (orange) calcium levels provided to yeast cells with calcitriol (CAL), control (CON) treated cells .Yellow denotes Glucose-deficient conditions.

	1	2	3	4	5	6	7	8	9	10	11	12
A	CAL	CON				CAL	CON					
B	CAL	CON				CAL	CON					
C	CAL	CON				CAL	CON					
D												
E												
F	CAL	CON				CAL	CON					
G	CAL	CON				CAL	CON					
H	CAL	CON				CAL	CON					

Table 7 Calcium Optimal Stress conditions: Stage 2 Plate set up

The table shows calcitriol treated yeast cells exposed to various calcium concentrations ranging from 3.2- 0 µg/ml.

	1	2	3	4	5	6	7	8	9	10	11	12
CAL	3.2	3.0	2.8	2.6	2.4	2.2	2.0	1.8	1.6			
CON	3.2	3.0	2.8	2.6	2.4	2.2	2.0	1.8	1.6			
MED	MED	MED	MED	MED	MED	MED	MED	MED	MED			
CAL	1.6	1.4	1.2	1.0	0.8	0.6	0.4	0.2	0.0			
CON	1.6	1.4	1.2	1.0	0.8	0.6	0.4	0.2	0.0			
MED	MED	MED	MED	MED	MED	MED	MED	MED	MED			

Table 8 Final Calcium optimal concentration: Stage 3 Plate Set up

The table shows a set of calcium concentrations ranging from 1.6-1.0 µg/ml.

	1	2	3	4	5	6	7	8	9	10	11	12
CAL	1.6	1.5	1.4	1.3	1.2	1.1	1.0					
CON	1.6	1.5	1.4	1.3	1.2	1.1	1.0					
MED	MED	MED	MED	MED	MED	MED	MED					
D												
E												
F												
G												
H												

4.3.2 Fluorescent Cell imaging for Calcium Ion Transportation

After determining the optimum calcium concentration parameter, we elucidated the calcium ion transportation inside the cells by fluorescent imaging technique. Cell imaging by loading indo-1 pentapotassium dye l increases the fluorescence in accordance with emission and excitation spectra. The wavelength of emission/excitation spectra for this fluorescent dye is referred from the literature as 410/480 nm. However, the wavelength value was corrected according to our protocol setting with the help of a standard curve.

Procedure:

1. Two individual cell cultures with a cell density of OD_{600}=1 (i.e.; 1.5 x 10^7 cells/ml) are incubated overnight. One of the cell cultures is treated with calcitriol at 4:1 ratio and the other serves as a reference with normal cellular levels.
2. Cells are then harvested and centrifuged at 7500 rpm for 2 minutes.
3. The supernatant is discarded and the pellet is washed three times with plain media.
4. Sample 1 without calcitriol: 10^9 cells /ml of the sample 1 is loaded into each of 1ml centrifuge tube and this step is also repeated to sample 2 containing calcitriol.
5. Finally, 32 samples each with 10^9 cells/ml are prepared; in which 16 samples are treated with calcitriol and the other 16 samples contain no calcitriol.
6. From 16 samples each, 8 samples were loaded with indo-1 pentapotassium dye using a loading buffer (composition discussed in Appendices).
7. Similarly, the remaining control samples are treated with another loading buffer that contains no dye within them.
8. All the samples are incubated for 90 minutes at a temperature of 30° C
9. After incubation, the cells in the samples are washed and centrifuged again at 7500 rpm for 2 minutes.
10. The washing buffer is then added to the samples and incubated for 30 min at 0°C.
11. Transfer aliquots of 0.2 ml from each sample and add 3 ml of washing buffer (composition discussed in Appendices).
12. Finally, indicated calcium concentration is added to the final concentrated samples.
13. Analyze the sample with the indicated calcium concentrations of 0.5M, 0.25M, 0.125M, 0.0625M, 0.0312M, 0.0156M, and 0.0078M

14. Aliquots of the treated samples are removed for fluorescent measurement (Isolate 1)
15. After then, the treated samples are filter sterilized with membrane pore size of 0.2µm and the filtrate is added with that of control samples.
16. Aliquots of the control samples containing the filtrate are obtained (Isolate 2)
17. Isolate 1 and 2 are plated in a fluorescent detecting plate and they are measured in fluorescent Cytation Imaging Reader. According to Grynkiewicz et al [71], the fluorescence ratio for the dye indo-1 pentapotassium dye was proposed as 410/480 nm, respectively.
18. A standard curve for the indicated amount of calcium concentration with dye 1 is plotted.
19. R_{min} (free dye fluorescence ratio) and R_{max} (calcium saturated dye fluorescence ratio) are determined from the standard curve.
20. From the fluorescent readings obtained from isolate 1 and 2, the calcium ion concentration at normal cellular levels and in calcitriol-treated cells are evaluated.

4.4 Genomic analysis for calcium signaling networks

To better understand the genomic networks involved in the calcium signaling process mediated by calcitriol, we conducted the BLAST search. The genome sequence for the BLAST searches are obtained from Uniprot database. The screened mutants are experimented with calcitriol using a yeast gene deletion library array.

4.4.1 Gene Deletion Library

A set of 384 individual strains constituting 4700 MATa haploid gene deletion strains of *Saccharomyces cerevisiae* (yeast) originally derived from BY4741 were prepared in 16 plates. These mutant plates are produced by hand-pinning sets. For our purpose, we selected certain mutants from the gene deletion sets that were originally prepared from Dr. Myron Smith Lab as depicted in figure 4 [72]. The screened mutants were then picked and streaked over a YPD agar plate. These plates were incubated for two days at optimal conditions that allows the growth of mutant colonies which are devoid of their respective genes. The picked and isolated colonies from the gene deletion plates are listed in table 9.

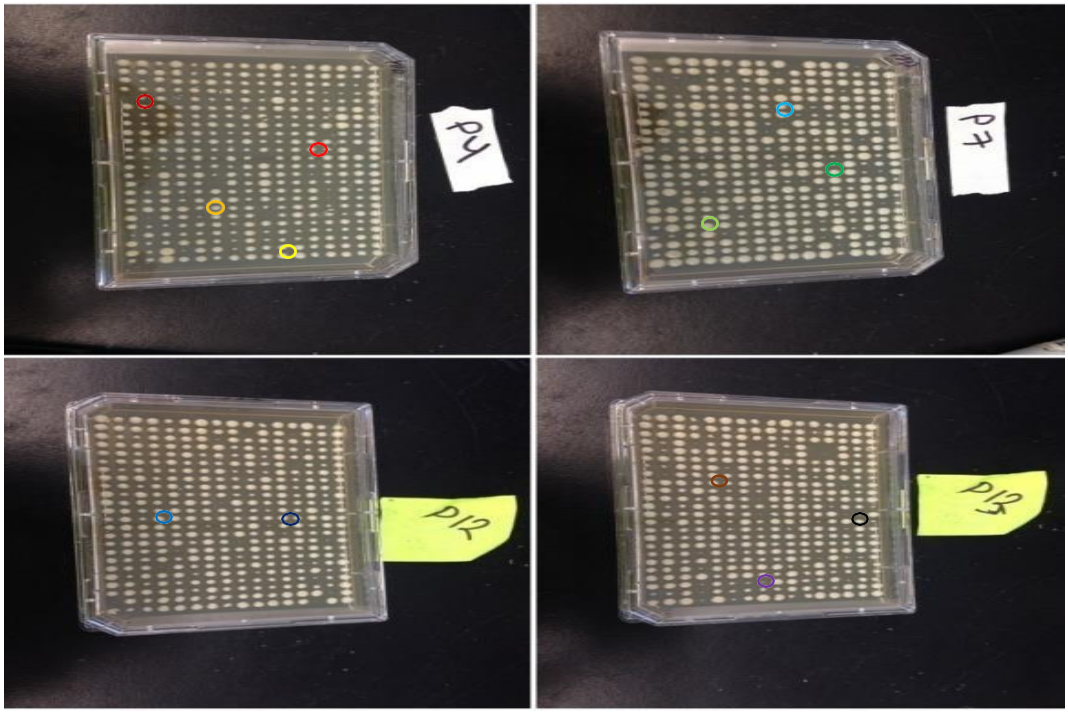

Figure 4 Yeast Deletion Genome Array with set of deleted genomic strains

The figure displays the selected genomic strains from the yeast deletion genome array and their respective functions as listed in table 9

Table 9 Genomic Strains

Marker displayed in figure 4	Gene Name	Strain Name	Function of the gene
○	CYM1	YDR430C	Conduct Protein Degradation and a metalloprotease
○	YVC1	YOR087	Vacuolar calcium transporter/ Only Human Mimicking Protein
○	SNF4	YGL115W	Activates Glucose Metabolism and initiates DNA replication
○	CCH1	YGR217W	Calcium Influx Response Mediator
○	MNE1	YOR350C	Mitochondrial Protein Transcription process
○	PMC1	YGL006W	Regulates Vacuolar calcium transportation
○	GAT4	IR013C	Cell membrane cleavage
○	CNB1	YKL190W	Stress Response Calcium Channel
○	IRC13	YOR235W	Functional Recombinant Protein
○	ECM7	YLR443	Membrane Protein Calcium channel
○	MID1	YNL291C	ER mediated calcium channel
○	CRZ1	YNL027W	Nuclear Calcium Transcription Factor

After the cultivation of genomic strains in agar plates, the cells were further sub-cultured in a broth culture with OD 0.5 (1.5×10^7 cells /ml). Following that, the corresponding genomic strains are further treated with calcitriol under the optimal calcium concentration range obtained in the previous analysis. It is conducted to test the efficacy of calcitriol against these genomic strains, which helps elucidating the role of these analyzed genes in calcitriol functioning. The study design is explained in table 10 and 11.

Table 10 Genomic Analysis Plate Set up 1

The table shows the calcitriol (CAL) and control (CON) treatment on selected genomic strains grouped under two sets followed in table 11.

Genomic Strains	1	2	3	4	5	6	7	8	9	10	11	12
YVC1	CAL	CAL	CAL	CON	CON	CON						
CCH1	CAL	CAL	CAL	CON	CON	CON						
PMC1	CAL	CAL	CAL	CON	CON	CON						
CNB1	CAL	CAL	CAL	CON	CON	CON						
ECM7	CAL	CAL	CAL	CON	CON	CON						
CRZ1	CAL	CAL	CAL	CON	CON	CON						

Table 11 Genomic Analysis Plate set up 2

The table shows the calcitriol (CAL) and control (CON) treatment on selected genomic strains

Genomic Strains	1		2	3	4	5	6	7	8	9	10	11	12
CYM1	CAL		CAL	CAL	CON	CON	CON						
SNF4	CAL		CAL	CAL	CON	CON	CON						
MNE1	CAL		CAL	CAL	CON	CON	CON						
GAT4	CAL		CAL	CAL	CON	CON	CON						
IRC13	CAL		CAL	CAL	CON	CON	CON						
MID1	CAL		CAL	CAL	CON	CON	CON						

4.5 Calcemic Effects of Calcitriol

From the above series of experiments, one would conclude that there should be a direct relationship persisting between calcium concentration and calcitriol treatment. In accordance with the hypothesis developed from our literature survey (described in chapter 3), we experimented on the calcemic effects caused by calcitriol in the cellular levels by an anaerobic model set up. We developed two distinct models based on anaerobic study and amino-acid shock analysis.

4.5.1 Anaerobic Modelling

The mechanism of developing an anaerobic set up included the use of atmosphere generation systems. For the generation of such atmosphere, we sought the help of AnaeroGen 3.5L (Code N: AN0035A) purchased from Thermo Scientific Fisher Ltd and anaerobic indicator purchased from the same (Code No: BR005B). AnaeroGen sachet essentially contains ascorbic acid and rapidly generates the anaerobic environment by sealing it within a plastic anaerobic jar. The sealing of the jar allows the rapid absorption of atmospheric oxygen with the simultaneous production of carbon dioxide.

An example of the setup is displayed in figure 5. Along with the use of atmosphere generation system, we implemented an Oxoid anaerobic indicator that allows the identification of anaerobic conditions achieved and maintained inside the jar. The resulting oxygen level in the jar reaches to 1% within 30 minutes and CO_2 levels up to 13%. It is denoted by the change in color from pink to white which indicates the anaerobic conditions.

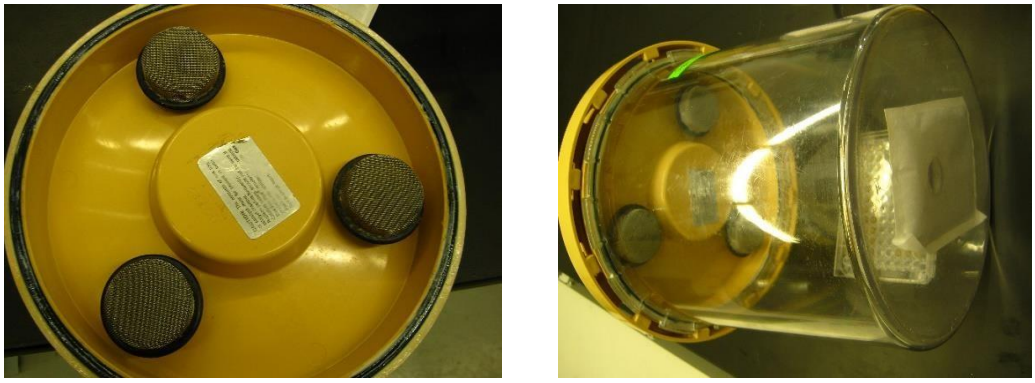

Figure 5 Anaerobic Chamber Modelling

Figure 5 displays the anaerobic suction clamp on the left and the experimental set up on the right

Procedure:

1. We followed the same protocol as explained before but at anaerobic conditions.
2. The plates for anaerobic cell growth are set up with calcitriol/non-calcitriol treated group along with a reference plate maintained under aerobic conditions.
3. The results might possibly help to determine the oxygen affinity of the calcitriol.

4.5.2 Aspartate–Glutamate Shock Analysis

The second part of our study is to understand the role of amino acids that might have an impact in the calcium signaling effects of calcitriol. As discussed in chapter 3, aspartate and glutamate are two main amino acids contained in the EF binding motif that could trigger the calcium signaling responses in calcitriol treated yeast cells. To elucidate this relationship, we developed an aspartate – glutamate enriched medium that could provide an amino acid shock response over the normal cellular growth

4.6 Validation of the results

The final segment validates the results that were obtained in the previous sections of our study. To validate the results, we initially conducted an anaerobic dye loading set up with normalization of cells in anaerobic conditions. We followed the same procedure as explained in section 4.3.2 but under anaerobic conditions. Here we deduced the calcitriol-mediated calcium ion transportation during anaerobic yeast growth.

4.6.1 Oxidative Stress Analysis

We tested our hypothesis based on oxidative stress response analysis depending upon the free radical counteractive mechanisms of calcitriol. For this purpose, we employed UV-A irradiation and AAPH.

4.6.2 UVA irradiation Analysis

We developed an UV-A irradiation exposure set up. The set up consists of a timing gauge which allows setting of a time interval used for this study. We used three UV fluorescent tubes, the F20T12/BLB (20W T12 (T10) Fluorescent Black-light Blue Medium Bi-Pin Base). The UV wavelength produced by this tube is at the range of 368 nm which comes under UVA band wavelength. The entire exposure set up is portrayed in figure 6 and it is built under room temperature conditions.

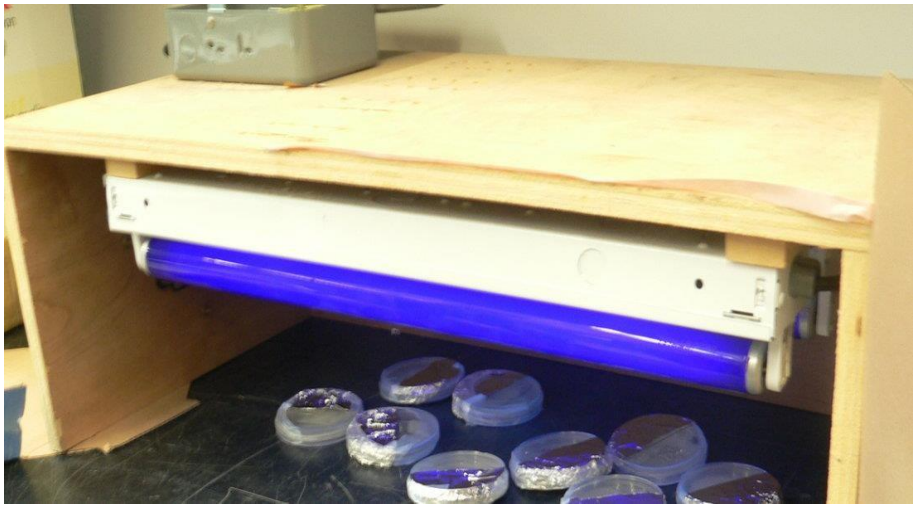

Figure 6 UV-A irradiation Exposure Set Up

Procedure:

1. We used a 96 well plate set up in this study.
2. We first used the agar plate technique to spread 10^9 cells /ml over the agar surface by a spread plate technique. The technique allows the uniform spreading of yeast cells by a hockey stick. With a reference dish, we treated one agar plate with 30 µl of calcitriol and it is uniformly distributed over the surface of the plate. However, these results are omitted due to ineffective data obtained at the end.
3. The second technique allows the plate set up with the broth culture containing calcitriol containing cells and control treated cells kept under UV-A exposure at different time intervals.
4. The final results should deduce the calcitriol anti-oxidant property to elucidate the generation of free radicals in the yeast cellular system.

4.6.3 AAPH

For our model, AAPH is used as an effective chemical agent to induce oxidative stress. It is used at a concentration of 50 mm [66]. The generation of free radicals under AAPH influence in yeast cells is measured at different time intervals. The final results of calcitriol functioning in counteracting AAPH free radical generation on yeast system are discussed in chapter 5.

4.6.4 Aging Model

Each section in this model deliberately tries to evaluate the different rule of Vitamin D theory associated with cellular mechanisms. Then we have one main rulebook which is to understand the process of aging theory. This model will define the therapeutic effects of calcitriol-treated under aging/starvations conditions.

Procedure:

The procedure was carried out for a period of 21 days [69]. For this model, we developed a synthetic defined medium which is specifically used for chronological yeast aging studies. The media description is listed at the Appendices section.

1. Yeast culture, Strain S288C is streaked over an YPD agar plate and incubated at 30° C for 48 hours. After the incubation period, a single colony was picked and inoculated into a 5 ml YPD broth media.
2. It is incubated overnight by providing constant agitation in a shaker (temperature: 30^{o}C, agitation: 750 rpm)
3. 50 µl of the overnight culture is incubated with 5 ml of synthetic chronological life span media. This culture is again maintained at constant shaking for a period of 3 weeks till the completion of aging experiment.
4. In our first trail during 2 days of incubation, 5 µl of the cell culture kept in the shaker is removed and added with 145 µl of YPD media. Triplicate is reproduced with calcitriol and without calcitriol on yeast cells to determine the calcitriol effect over 2 day period of aging. The OD measurement was recorded to measure the count of live cells using a UV spectrophotometer.
5. Similarly, a record for the corresponding: days 2, 5, 8, 12, 15, 18, 21 days is obtained. Finally, seven age points are recorded in the three weeks period.

4.7 Conclusion

In this chapter, we developed an integrated method combining the bioinformatic approach, intracellular ionic stress response, fluorescent optical imaging, genomic drug profiling and anaerobic modelling. The oxidative stress analysis was evaluated by an anaerobic experimental set-up and by aspartate –glutamate shock analysis treatment to deduce the calcemic effects of calcitriol which has led to its limitation in chemotherapy/other generic diseases, as mentioned earlier.

The next chapter will show our results in terms of growth/concentration profiles /cell viability and in terms of fluorescent intensity. The results will be validated by experimenting model organisms on different hypothesis as referred from the literature.

Chapter 5. Results

The results for the corresponding experiments mentioned in chapter 4 are reported and elaborated in this chapter.

5.1 Molecular Docking Results

The results from molecular docking simulations are provided in table 12 and the corresponding docked pictures obtained from the software are depicted in figure 7. The figure displays the list of docked proteins Mid1 (PDB ID: 4XOH), VCX1 (PDB ID: 4K1C), CMD1 (PDB ID: 4DS7), SNF4 (PDB ID: 2NYC), YVC1 (PDB ID: 2PNN), TRPA1 (PDB ID: 3J9P) with the respective ligand calcitriol. From analyzing the table 12, the prediction of average connecting pairs varies from 21.13 to 17.86 base pairs overall, which displays the interconnectivity of calcitriol with the docked yeast channel proteins. Similarly, the total energy simulated during these binding interactions ranges from -85.51 to -75.30. The results provided in table 12 clearly show the lower binding energies required for the protein interactions. The negative nature of these interactions depicts the lower consumption of ATP energy needed for the overall molecular protein interactions with calcitriol. Further, the data achieved excellent agreement with human body interactions which similarly requires less energy frequency for protein binding interactions. In conclusion, the negative nature of total binding energy column shown in table 12 predicts the high binding affinity of calcitriol with that of calcium channel proteins inside the yeast system. This further indicates that yeast cells provide a supporting platform for calcitriol mediated interactions with the calcium channel proteins.

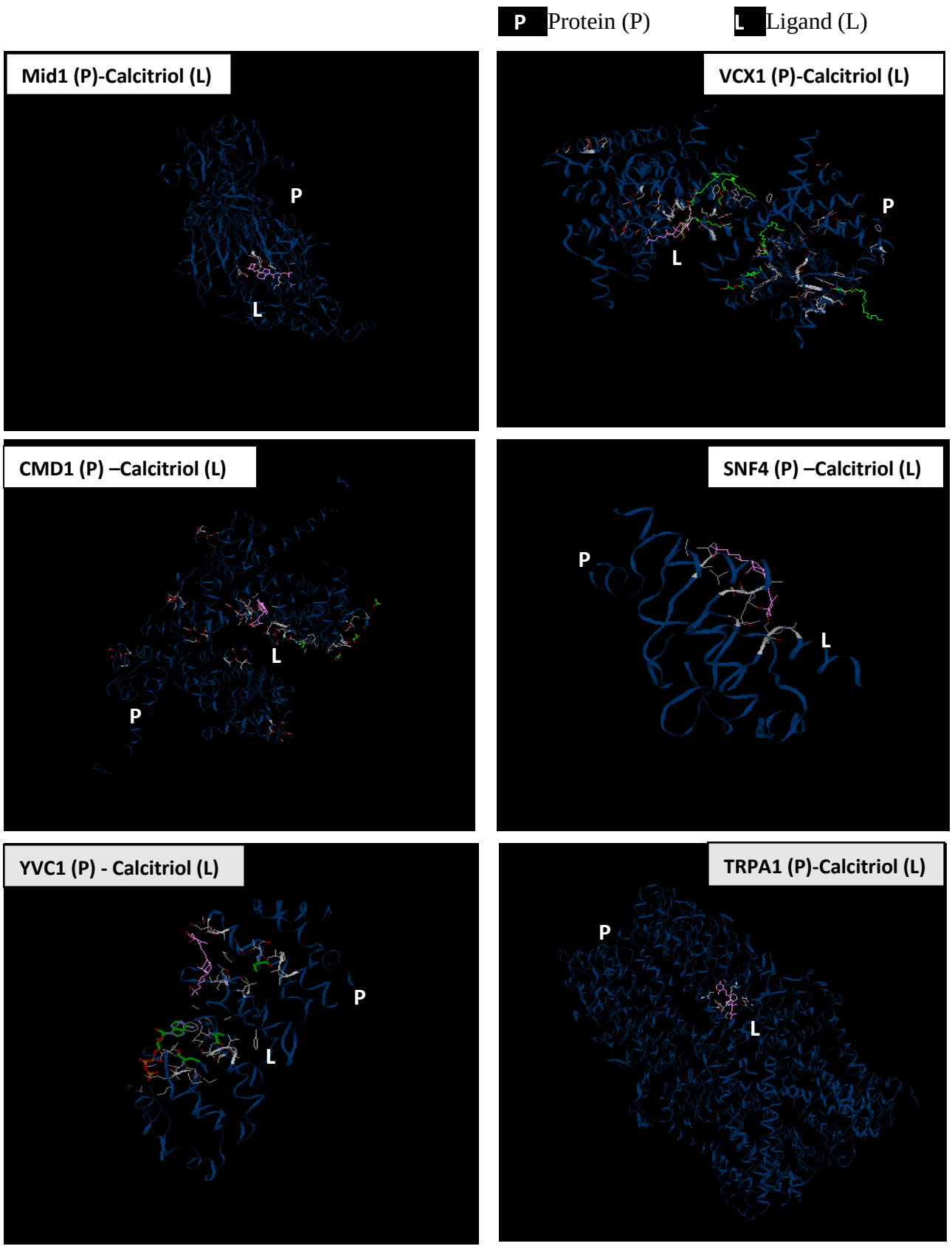

Figure 7 Docking Simulation Results; Protein Interactions

Displays the final docking images of the yeast calcium transporters (P) with that of calcitriol (L)

Table 12 Binding Energy Evaluations for the Simulated Models

The table lists the final predicted values from the simulation results.

S .No	Protein-Ligand Interaction	Total Energy (ΔG)	Average Connecting Pairs
1	MID1-Calcitriol	-85.51	17.86
2	VCX1-Calcitrol	-83.66	19.56
3	CMD1-Calcitrol	-79.17	19.86
4	SNF4-Calcitrol	-78.74	18.90
5	YVC1-Calcitrol	-75.30	16.10
6	TRPA1-Calcitrol	-79.13	21.13

5.2 STRETCHER

According to the docking simulations based on the protein interactions in yeast, we conducted a genome sequence analysis for the docked proteins. The results of the STRETCHER alignment of the corresponding proteins are described in table 13. The data provided in the similarity column in the table shows an approximation of list of obtained sequence matches with yeast calcium channel proteins and human receptor. The overall sequence percentage column in similarity scoring function for the respective proteins MID1, VCX1, CMD1, SNF4, YVC1 are found as 28.8, 28, 18.3, 31.2 and 27.2. These scoring functions provide a conclusive evidence for sequence matches occurring between the analyzed pair of proteins. It also determines the number of identical sequences present in-between them. However, the data displayed in identity column provides the exact match of protein sequences resulted in a weak association of sequence matches in-between these proteins. The data for the respective proteins ranges from 16.2, 3.8, 9.6, 14.7, and 14.3. However, it is reliable from the fact that human genome sequences responsible for calcitriol binding are still present, even in negligible number, in these analyzed matches.

Table 13 Sequence Matching Results from STRETCHER tool

The table displays the identity and the similarity of the matching sequences between the calcitriol receptor and yeast proteins. Identity displays the matching sequences without any gaps. Similarity is the overall matching of sequences based on similar R-group characteristics.

S. No	STRETCHER Aligned Sequences	Identity		Similarity		Total Sequence Length
		Matched Sequences	%	Matched Sequences	%	
1	Yeast MID1 –Human Calcitriol Receptor	89/548	16.2	158/548	28.8	548
2	Yeast VCX1-Human Calcitriol Receptor	60/435	3.8	122/435	28.0	435
3	Yeast CMD1- Human Calcitriol Receptor	41/427	9.6	78/427	18.3	427
4	Yeast SNF4- Human Calcitriol Receptor	63/430	14.7	134/430	31.2	430
5	Yeast YVC1- Human Calcitriol Receptor	97/677	14.3	184/677	27.2	677

5.3 Pharmacokinetic Drug Profiling Results

To understand the pharmacokinetic functions of the drug, we conducted MIC analysis to determine the minimum inhibitory concentration of the drug. For this purpose, we used a drug concentration of 0.50 µg/l at the start of the experiment. After repeating MIC tests over 3-4 times, we found out that there was no minimal inhibition occurring in the growth of cells.

In table 14, the orange values denote the calcitriol treated group and the purple values represent the control treated group. From the data analyzed, we estimated that there was an enhancement occurring in the growth of yeast cells when they are treated with calcitriol and their OD_{600} readings varied from 1.991 to 1.844, whereas the control cells displayed a minimal growth rate recording an OD_{600} reading of 1.481 to 1.336. This antibiotic sensitivity test provides with a conclusion that yeast cells grow at a faster rate under the presence of calcitriol. In table 14, the columns A1-6, B1-6, C1-6 in the 96-well plate contains triplicates of yeast cells treated with calcitriol, whereas the wells D1-6, E1-6, and F1-6 contain control cells without any drug treatment.

It is clearly shown from the table 14, that the former wells (A, B, C) with calcitriol treatment show higher growth rate over a 24 hour incubation period as compared to the latter analysed wells (D, E, F). This allows the predictability that calcitriol might function as a cell growth enhancement agent at optimum conditions.

Table 14 MIC Test OD_{600} values

The table shows the OD_{600} values at rows A-F and columns 1-6. Orange denotes the calcitriol treated cells and blue represents the control cells.

	1	2	3	4	5	6	7	8	9	10	11	12
A	1.991	1.932	1.926	1.901	1.866	1.858	0.076	0.089	1.755	0.058	0.054	0.055
B	1.979	1.929	1.919	1.9	1.852	1.866	0.062	0.114	1.74	0.045	0.059	0.053
C	1.977	1.927	1.905	1.895	1.846	1.844	0.112	0.149	1.765	0.047	0.051	0.055
D	1.481	1.462	1.352	1.421	1.46	1.44	0.069	0.07	1.53	0.064	0.05	0.042
E	1.483	1.456	1.4	1.336	1.45	1.49	0.057	0.069	1.472	0.075	0.05	0.052
F	1.452	1.489	1.512	1.479	1.422	1.467	0.051	0.046	1.416	0.046	0.05	0.045
G	0.08	0.07	0.084	0.075	0.07	0.059	0.056	0.051	0.064	0.049	0.048	0.053
H	0.051	0.081	0.055	0.054	0.053	0.049	0.069	0.047	0.054	0.051	0.047	0.049

5.3.1 MIC Data Prediction:

The data obtained from the MIC analysis validates the therapeutic protective functions of calcitriol. The yeast system referred as a human model here binds its proteins with calcitriol to establish an increased cellular metabolic mechanism inside the yeast cells leading to its higher growth rate. However, the protective mechanism of calcitriol by which this growth enhancement takes place is still a mystery.

5.3.2 Drug dependent concentration profiling

We believe that this growth enhancement mechanism is strongly coordinated with the calcium transportation based on our literature study. For this purpose, we determined the calcium related response of the drug.

5.3.3 Graphical Analysis using Gen5 Software Data analysis

The results for the stage 1 calcium related stress response yeast growth rates are plotted as curves using a Gen 5 Software data analysis [73]. From figure 8 under normal Ca^{2+} concentration conditions, the cells that are treated with calcitriol showed a visible enhancement in the growth of cells ranging from an OD of 0.8 – 1.8 during the time interval 12 – 16 hours of a total 24 hour growth period, whereas the control group had an OD range of 0.6-1.6. As we can see this from figure 8, the red curve which displays the calcitriol growth pattern represents higher growth rate when compared to the green curve that illustrates the control growth pattern. In contrast to this, when yeast cells are introduced to calcium deficient conditions as seen in figure 9, the calcitriol-treated group showed less growth rate with OD value ranging from 0.1-0.3, on the other hand, the control group displayed an OD range of 0.050 – 0.5. From these results, we realize that calcitriol becomes toxic and inhibit the cell growth under abnormal calcium conditions. This pattern is clearly represented in figure 9 which depicts the decline of growth pattern in calcitriol-treated cells (red curve) when compared to the control set of cells (green curve). Interestingly, the same is repeated even in the calcium rich conditions as portrayed in figure 10. Here, an irregular pattern of cell inhibition occurs during the log phase of calcitriol-treated group as compared with the control set group by OD difference ranging from 1.6-0.8 at 24 hour growth period. When we tested a similar hypothesis on glucose deficient conditions, we found out that calcitriol becomes completely toxic inhibiting the growth of yeast cells at OD 1 itself. This can be clearly seen in figure 11. These results conclude that the imbalance occurring in cellular calcium/ glucose homeostasis alters the functionality of calcitriol to react either toxic or as an enhancing agent.

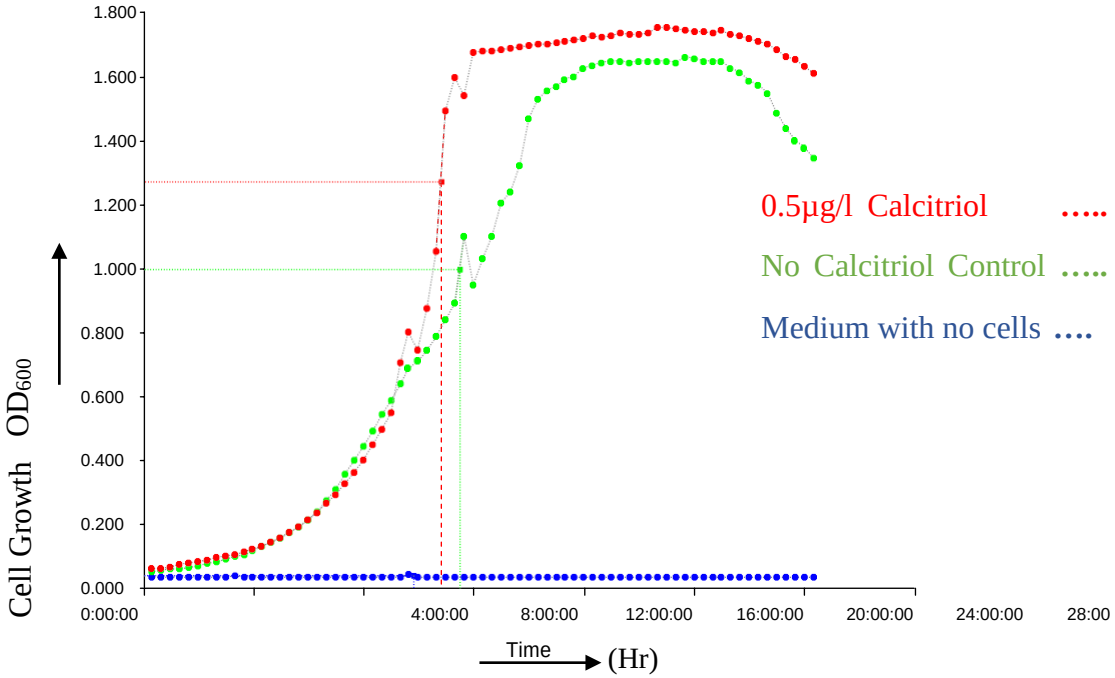

Figure 8 Normal Calcium Stress Response Curve

This figure displays the calcitriol and control treatment on yeast cells under normal calcium conditions

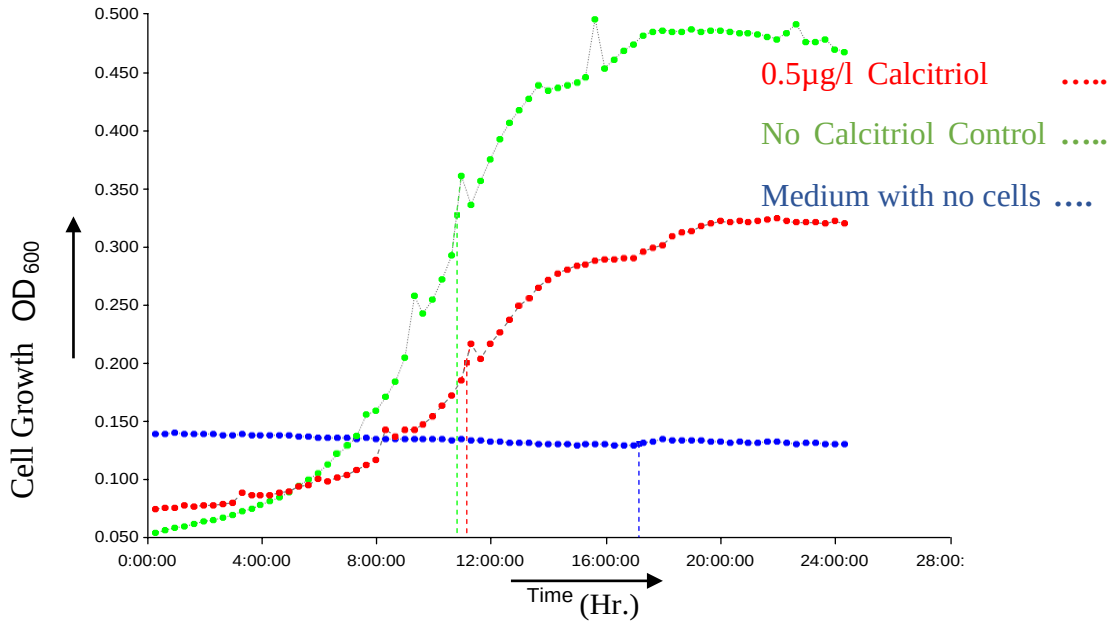

Figure 9 Calcium Deficient Stress Response Curve

This figure displays the calcitriol and control treatment on yeast cells under calcium deficient conditions

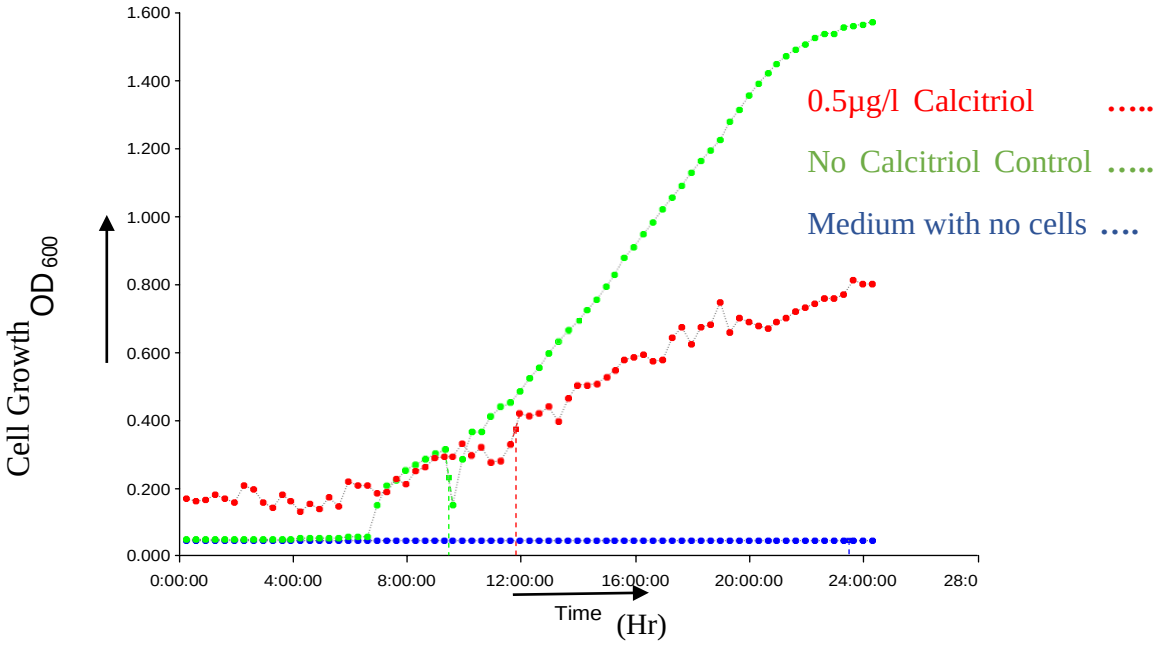

Figure 10 Excessive Calcium Stress Response Curve

This figure displays the calcitriol and control treatment on yeast cells under excessive calcium conditions

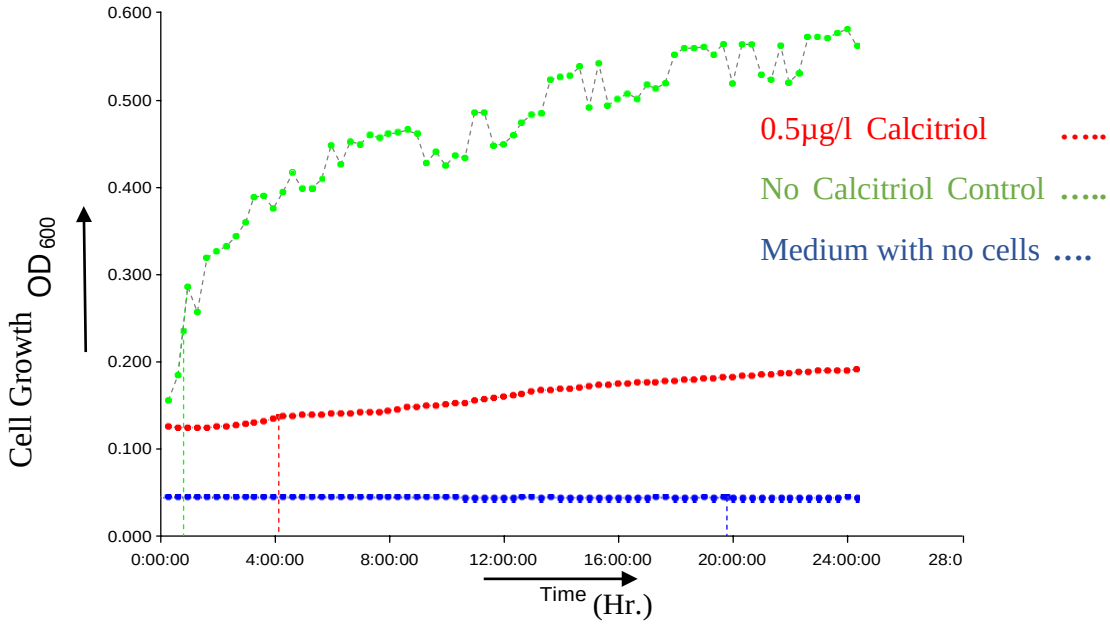

Figure 11 Glucose Deficient Stress Response Curve

This figure displays the calcitriol and control treatment on yeast cells under glucose deficient conditions

5.4 Optimum Drug Concentration Analysis

To address the above-seen calcium regulated inhibition/ enhancing effect in calcitriol treated yeast cells, we conducted a series of calcium concentration stress response analyses. The higher calcium concentration range is twice the normal range of optimum calcium concentration generally present in yeast cells; its value is 3.2 x 10^{-5} µg/ml Ca^{2+} concentration and the minimum calcium concentration is extended to 0 x 10^{-5} µg/ml Ca^{2+} concentration. The plate setup description for various cellular calcium concentrations is explained in Appendices section.

5.4.1 Interpretation of Results

The results for determining the optimum calcium concentration profiling to obtain higher calcitriol activity is provided in figure 12. The x-axis contains the calcium concentration (µg/ml) and y-axis display the OD average of cellular growth rate both in calcitriol and control treated groups. The red curve denotes the calcitriol treated cells whereas the blue curve represents the control treated cells in figure 12.

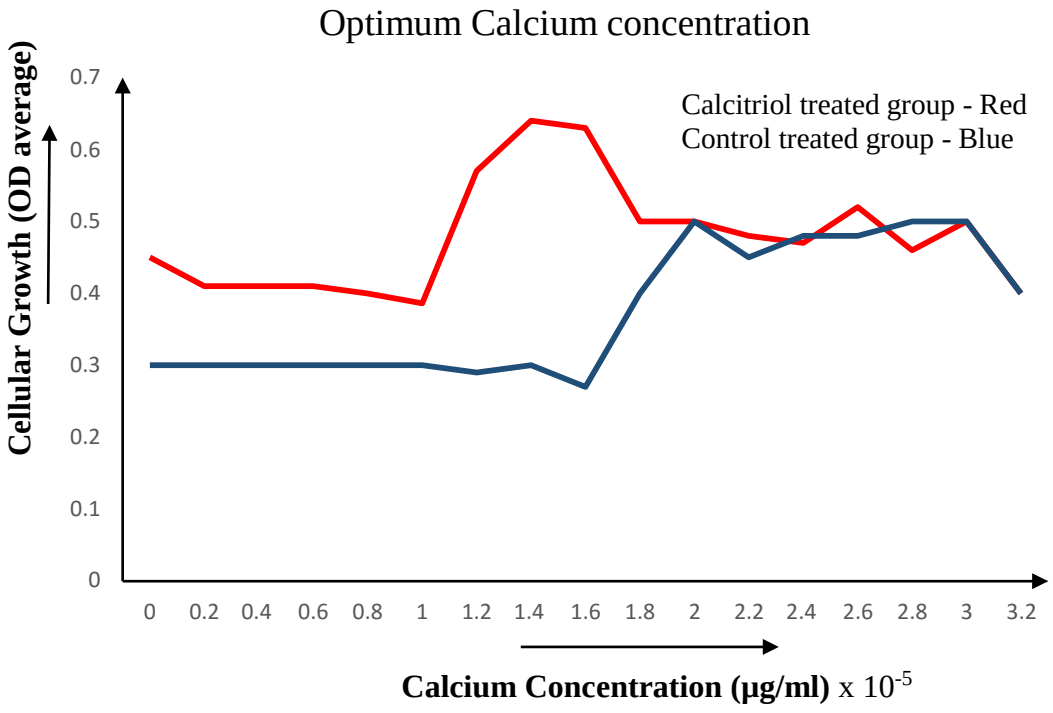

Figure 12 Optimum calcium concentration for cells grown with or without calcitriol

Figure shows the calcitriol and control treatment on yeast cells under various calcium concentrations ranging from 0 to 3.2 x 10^{-5} µg/ml. Here, peak effect of calcitriol on growth is seen at 1-1.6 µg/ml x 10^{-5} calcium concentration.

The above graph analyses the calcitriol effect on the growth of cells at different calcium concentrations. The results in the graph are assessed to determine the toxic /protective functions of calcitriol. Overall, from the above-conducted analysis, we see a distinct growth pattern occurring at different calcium concentrations. There is a large amount of growth enhancement in calcitriol treated group occurring in these calcium concentrations with an OD difference ranging from 0.1 to 0.37 OD units distinctly, i.e. OD (calcitriol) vs OD (no calcitriol). On the other hand in control treated group, a linear growth pattern is seen at calcium concentrations ranging from 0 - 1.8 µg/ml, however we can see an elevation in growth occurring at 1.6-2.2 x 10^{-5} µg/ml calcium concentration range, with a gradual reduction at the highest calcium concentrations. Also evident is that there is a certain amount of toxicity occurring at higher calcium concentrations from 2.2-3.2 x 10^{-5} µg/ml Ca^{2+}, when calcitriol is present. This is clearly represented from the diminished growth pattern obtained in these calcium concentrations.

Finally, we conclude that the optimum calcium concentration range for a positive calcitriol effect in the yeast system occurs at the calcium concentration range of 1.0-1.6 x 10^{-5} µg/ml.

5.4.2 Optimum Calcium Concentration

We again fine-tuned the optimized drug calcium concentration to a range of concentration from 1.0 to 1.6 x 10^{-5} µg/ml calcium concentration, with a step size of 0.1 µg/ml calcium concentration, similar to previous analysis. The parameters for the graphical analysis are followed as before. However, we followed an individual growth analysis for every single calcium concentration to determine the optimum calcitriol mediated calcium concentration as depicted in figure 13.

1.6 µg/ml Calcium Concentration

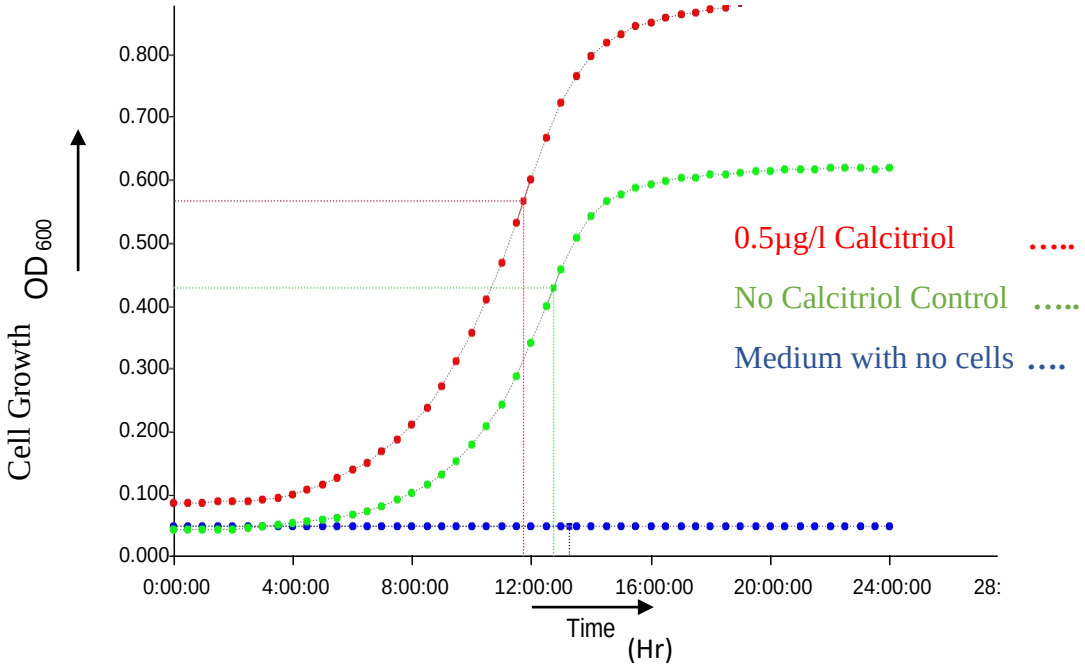

1.5 µg/ml Calcium Concentration

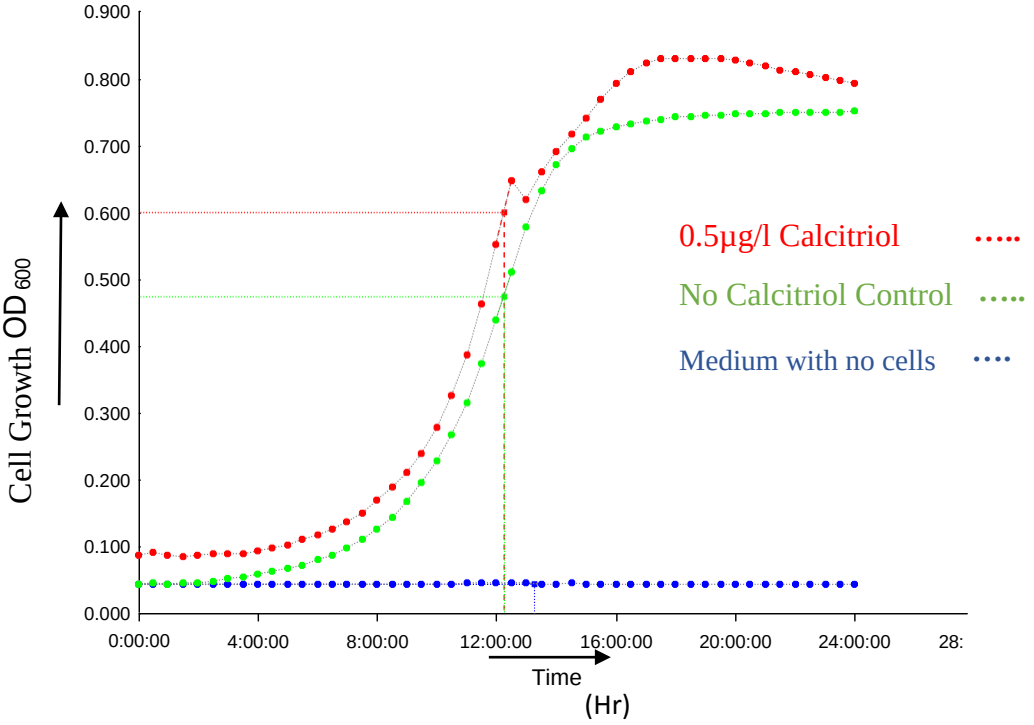

1.4 µg/ml Calcium Concentration

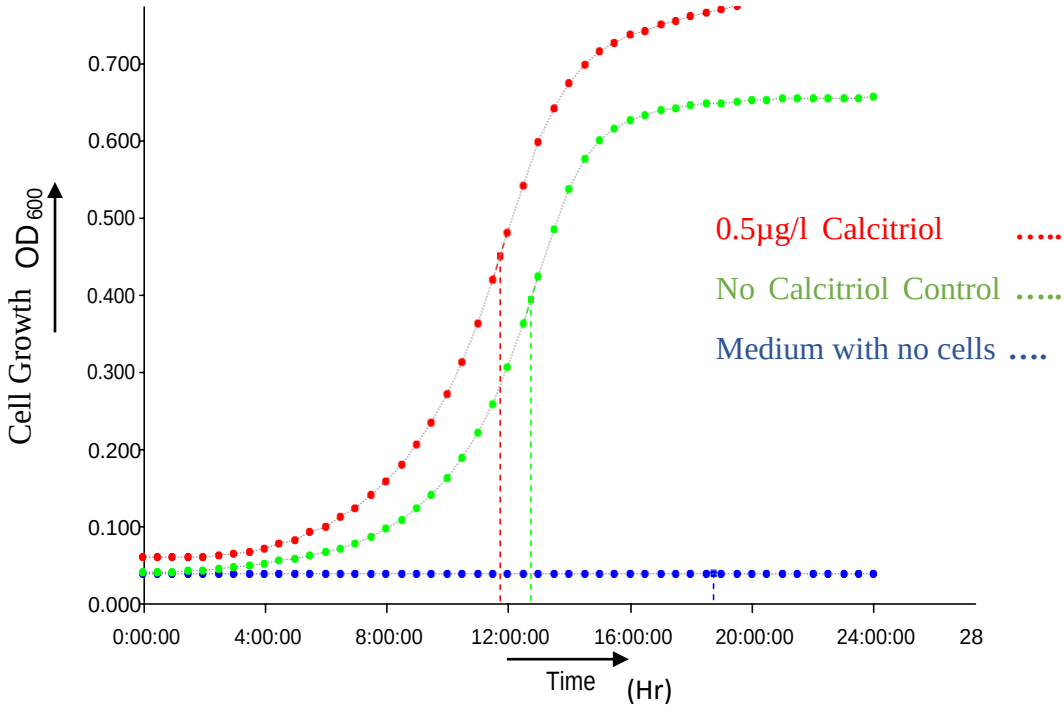

1.3 µg/ml Calcium Concentration

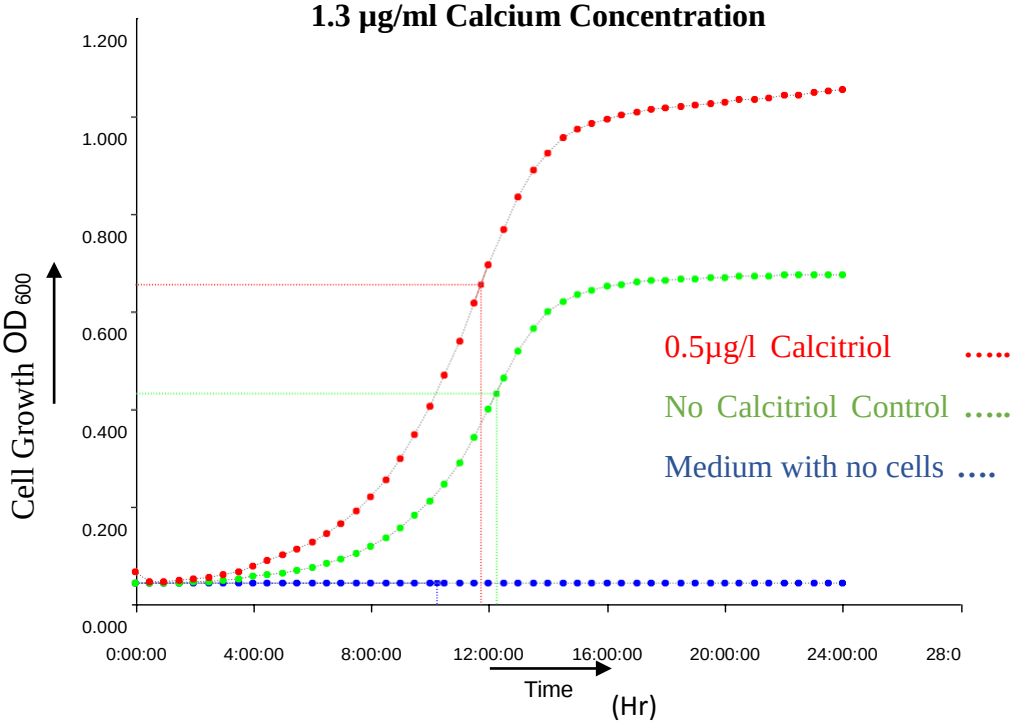

1.2 µg/ml Calcium Concentration

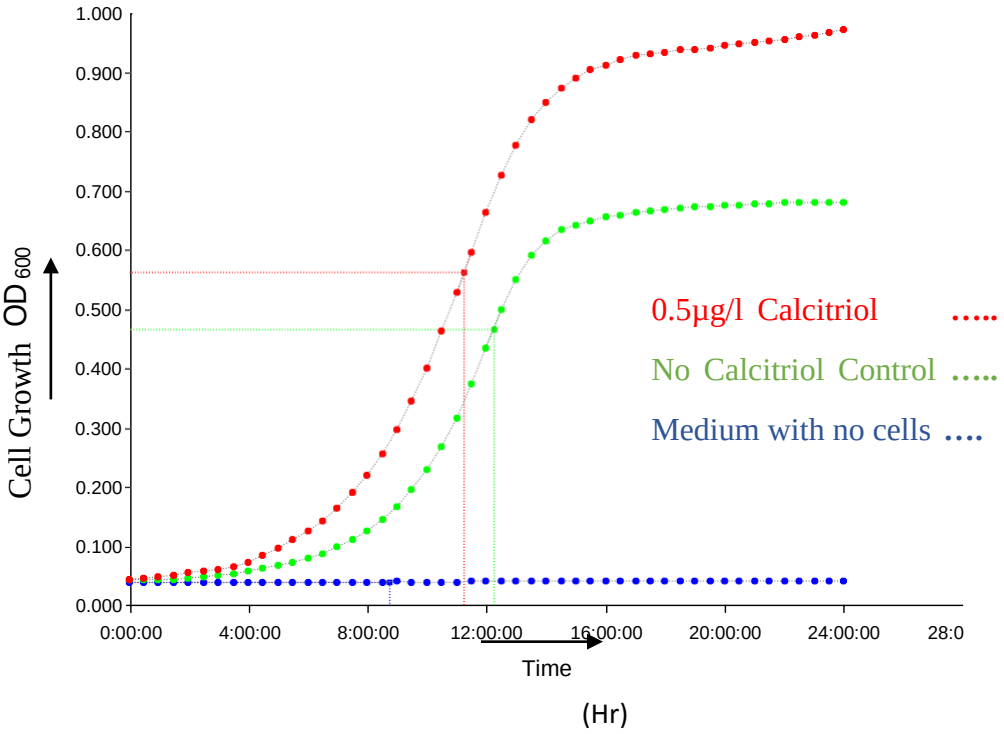

1.1 µg/ml Calcium Concentration

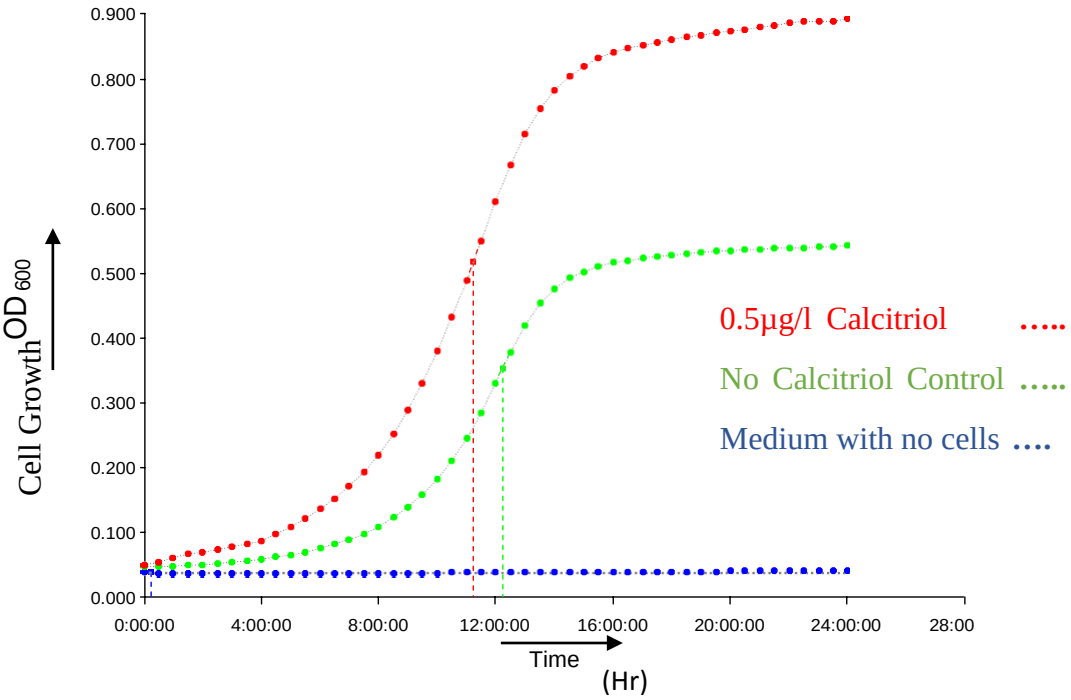

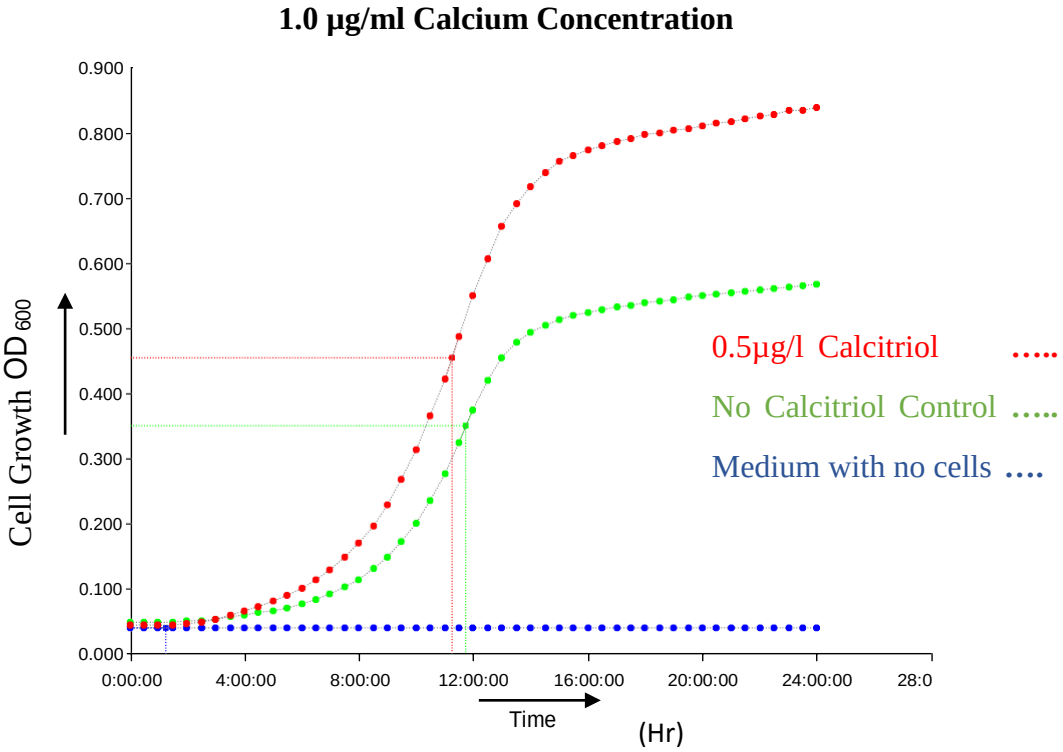

Figure 13 Final Stage of Calcium concentrations Analysis

The above set of graphs display yeast growth with or without calcitriol at different Ca^{2+} Concentrations ranging from 1.6- 1.0 x 10^{-5}µg/ml. optimal calcitriol effect occurs at 1.1 x 10^{-5}µg/ml calcium concentration.

In the above conducted graphical analysis, we can see that there was an increase in the growth of cells treated with calcitriol under these calcium concentrations. At the corresponding calcium concentrations of 1.0 µg/ml, 1.1 µg/ml, 1.2 µg/ml, 1.3 µg/ml, 1.4 µg/ml, 1.5 µg/ml, 1.6 µg/ml, the OD_{600} values for calcitriol and control treated group are 0.88(calcitriol)-0.56(no calcitriol), 0.91(calcitriol)-0.52(no calcitriol), 0.98(calcitriol)-0.71(no calcitriol), 1.13(calcitriol)-0.64(no calcitriol), 0.75(calcitriol)-0.62(no calcitriol), 0.78(calcitriol)-0.45(no calcitriol), and 0.84(calcitriol)-0.60(no calcitriol) respectively. We finally determined that maximum calcitriol activity was found at 1.1 µg/ml calcium concentration. However, other graphs show OD activity similar to this concentration, but the significance of calcitriol activity is visibly higher at this particular calcium concentration. Therefore, we conclude that 1.1 x 10^{-5} µg/ml calcium concentration is the optimum calcium concentration for calcitriol activity in the yeast cellular system.

5.5 Imaging Calcium Ion Transportation

To understand the calcium ion transportation occurring at this particular calcium concentration that causes elevation in the growth of yeast cells, we imaged yeast cells using fluorescent detection at a fluorescence ratio 410/480 nm, respectively.

5.5.1 Standard Curve

Initially, a standard curve is plotted using EGTA-Ca^{2+} Buffer solution. We analyzed the standard curve for the known calcium concentrations namely, 0.5M, 0.25M, 0.125 M, 0.0625M, 0.0312M, 0.0156M, and 0.0078M. The results are displayed in table 15. The standard imaging graph is plotted in figure 14.

Table 15 Standard Curve Fluorescence Detection
The table lists the standard values obtained from the calcium imaging dye.

Calcium concentration Range (M)	Fluorescent intensity (counts per second)
0.5M	6.94
0.25M	4.28
0.125M	3.16
0.0625M	3.08
0.0312M	2.64
0.0156M	1.59
0.0078M	0.28

From table 15, we can measure the fluorescent intensity for the known calcium concentration range. The tabulated values are calculated from the emission intensity detected under the fluorescent detector. The recorded data provide details based on the fluorescence triggered by the dye under that particular calcium concentration range. The standard values are plotted as a graph in figure 14.

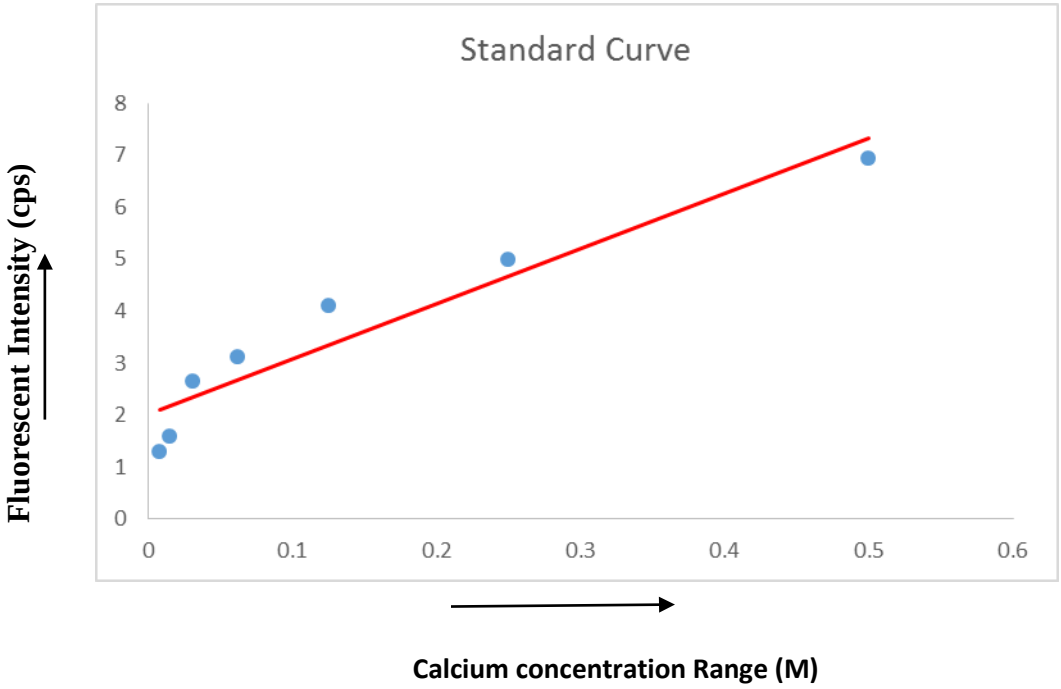

Figure 14 Standard Imaging Curve

The standard curve is plotted with known calcium concentrations ranging from 0.50M- 0.0078M, Y = 10.619X + 2.015

5.5.2 Calcitriol Mediated Intracellular calcium levels in Yeast

Based on the obtained standard graph, we evaluated the intracellular calcium levels in yeast cellular growth under calcitriol treatment. The amount of calcium ions bounded to the dye in calcitriol treated cells and control cells are calculated and listed in table 16.

Table 16 Aerobic Yeast Intracellular calcium during calcitriol treatment
The table displays the final intracellular calcium levels in calcitriol and control imaged yeast cells

Ca2+ Concentration (M)	**Calcitriol Imaged Cells (mM Ca^{2+} ions)**	**Control Imaged Cells (mM Ca^{2+} ions)**
0.5M	4.89	2.95
0.25M	2.45	2.94
0.125M	2.22	2.6
0.0625M	2.09	2.22
0.0312M	1.33	1.27
0.0156M	1.02	0.70
0.0078	0.913	0.375

The table provides the list of values obtained from the fluorescent detection using calcium imaging technique. The calcitriol treated cells at 0.5 M Ca^{2+} concentration range shows intracellular calcium level of 4.89 mM whereas the control cells showed intracellular calcium levels of 2.95 mM at the same calcium concentration. The values went on to decline gradually after the initial peak triggered in the calcitriol treated cells at 0.5M Ca^{2+} concentration. The value displayed at this Ca^{2+} concentration refers twice the range of normal cellular calcium levels. Interestingly, there is not much of change seen in other concentrations.

However, we can justify that sudden rise in cellular calcium concentration is due to the higher amount of calcitriol activity in 0.5 M Ca^{2+} concentration. The represented data in table 16 are plotted as a graph in figure 15.

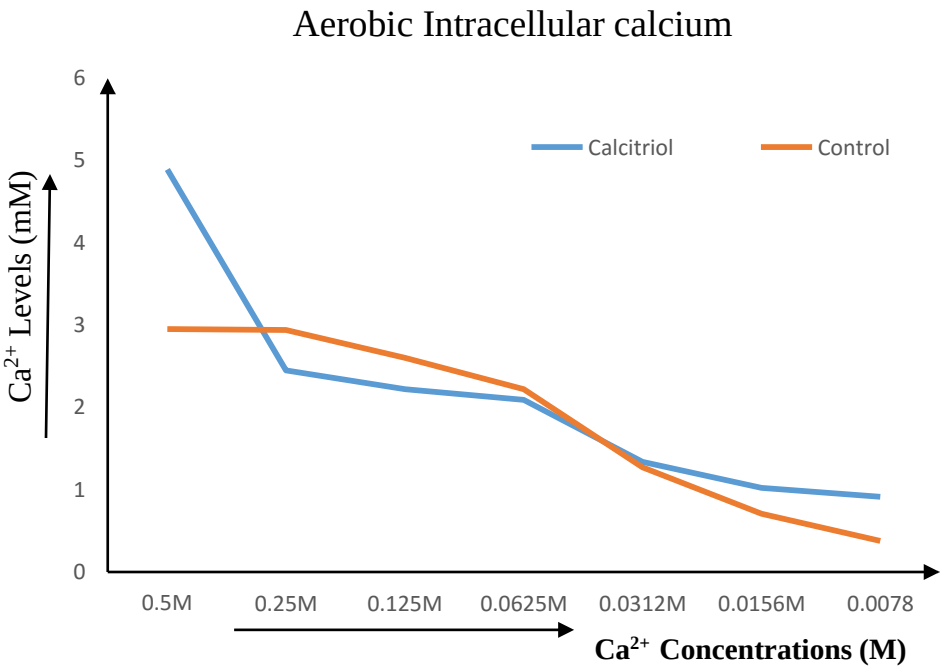

Figure 15 Intracellular Aerobic Calcium Levels

The graph displays the intracellular calcium levels in calcitriol treated and control cells in aerobic condition. Blue line representing the calcitriol activity shows higher peak range in intracellular calcium levels as compared with that of control cells (orange line)

In figure 15, the orange curve is the control treated cells and the blue curve depicts the calcitriol treated cells. From the graph, it is clear that calcitriol treated cells show an increased calcium concentration in the cytosolic compartment of the cell. This could be seen from the peak in the intracellular calcium levels at the low end of extracellular calcium examined. On the contrary, the control cells displayed a gradual decrease in intracellular calcium ions as extracellular Ca^{2+} concentrations increased. This further supports the idea of calcitriol mediated calcium regulation occurring within the yeast cells. However, there is still no conclusive finding regarding how this enhanced uptake of calcium is triggered by calcitriol inside the yeast system.

5.6 Genomic Analysis of the yeast model system

To get a better understanding of the calcium signaling mechanisms, we tried to investigate the roles of genomic regulation that may play an active role in these calcitriol mediated signaling mechanisms. For this purpose, growth was monitored using 12 yeast strains with gene deletions were treated with calcitriol at an optimum calcium concentration.

Two sets of six mutant each was set individually in a plate reader and monitored with an optical density wavelength of 600 nm for 24-hours to produce a growth curve. The results are displayed in figure 16 and table 17 provides the level of inhibition produced by calcitriol in the analyzed genomic strains.

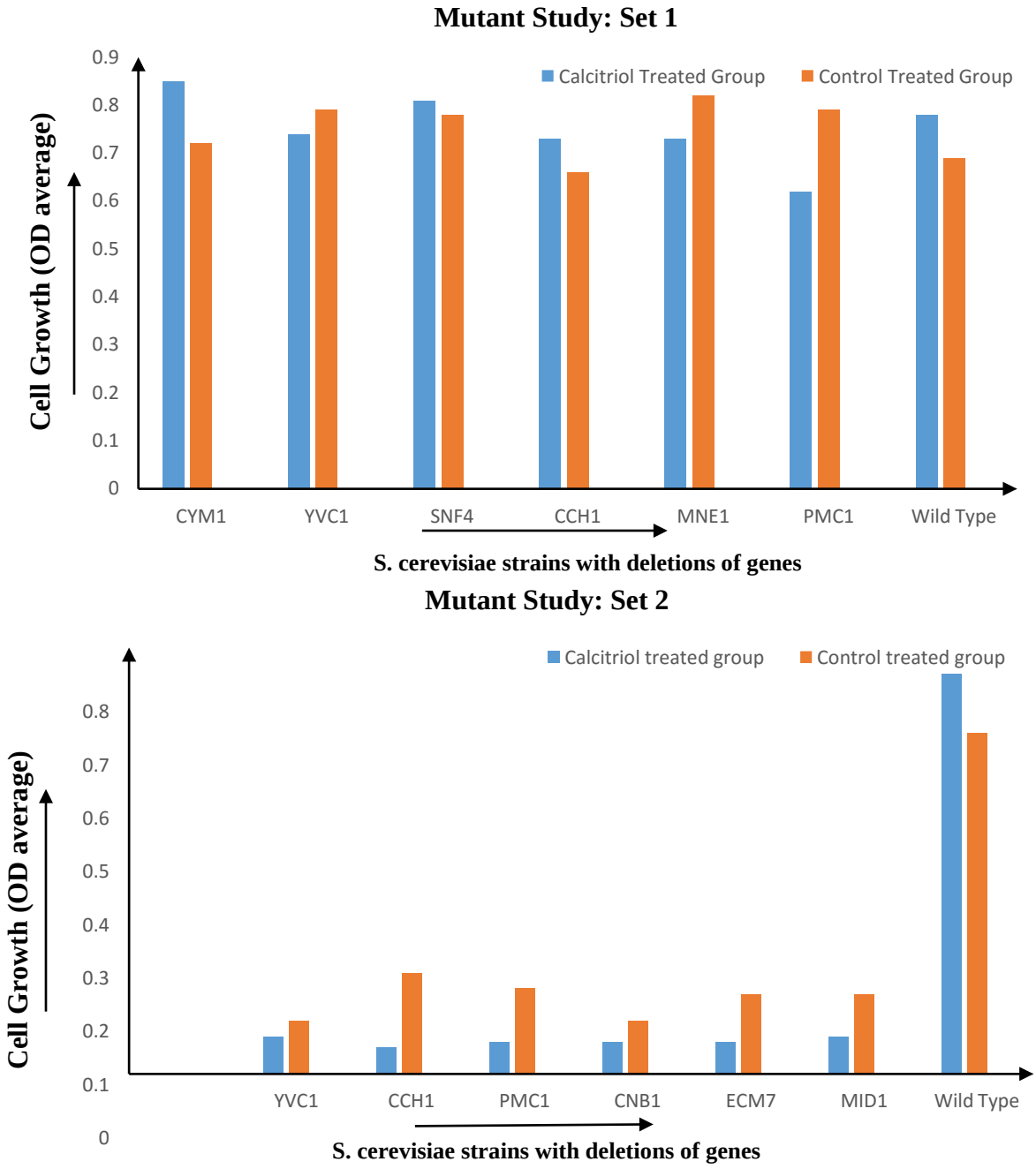

Figure 16 Growth Comparisons of Gene Deletion Strains

Figure displays the calcitriol effect on the 12 selected yeast strains with gene deletions as indicated

Table 17 Cytotoxicity effect of Calcitriol over Gene Deletion Strains

Gene deletion Strains inhibited at higher rate with calcitriol	**Gene deletion Strains inhibited minimally with calcitriol**
CYM1 / YDR430C (Vitamin D homolog)	Yvc1/ YOR087 (Ca2+ Pump-Random Strain)
SNF4 / YGL115W (Vitamin D homolog)	CCH1/YGR217W (Ca2+ Pump-Random Strain)
MNE1 / YOR350C (Vitamin D homolog)	PMC1/YGL006W (Ca2+ Pump-Random Strain)
GAT4 / YIR013C (Vitamin D homolog)	CNB1/YKL190W (Ca2+ Pump-Random Strain)
IRC13 /YOR235 W (Random Strain)	ECM7/YLR443 (Ca2+ Pump-Random Strain)
Mid1/YNL291C (Ca2+ Pump-Random Strain)	CRZ1/YNL027W (Ca2+ Pump-Random Strain)
Wild Type (No Inhibition occurred**)**	Wild Type (No Inhibition occurred)

The graphs in the figure 16 display the OD average of cell growth rate produced from calcitriol and control treatment in the tested genomic strains. It is clear from the graphs that set 2 mutant genomic strains provided a higher inhibition rate with calcitriol treatment when compared with that of control treatment. The inhibited gene deletion strains are listed distinctly in table 17 based on the rate of inhibition. From the overall study, CYM1, SNF4, MNE1, GAT4, IRC13, MID1 gene deletion strains display a higher order of inhibition towards calcitriol, whereas deletions of YVC1, CCH1, PMC1, CNB1, ECM7 and CRZ1 had a lower inhibition with calcitriol treatment. This shows the genes deleted in the most inhibited strains have an important role in calcitriol functioning as compared with that of less inhibited strains.

5.7 Anaerobic Model

Our developed hypothesis states that calcitriol Ca^{2+} signaling effects are mainly contributed by the oxygen affinity of the drug. The analysis was conducted under a range of Ca^{2+} concentrations as displayed in table 18 under aerobic and anaerobic conditions.

Table 18 Anaerobic Cell Growth Analysis

Calcium Concentration x 10^{-5} (µg/ml)	**Anaerobic (cells/ml)**			**Aerobic (cells/ml)**		
	Control(A)	**Calcitriol(B)**	**(B-A)/A**	**Control(A)**	**Calcitriol(B)**	**(B-A)/A**
1.6	0.287	0.315	0.097	0.428	0.724	0.691
1.4	0.27	0.33	0.222	0.404	0.683	0.690
1.2	0.267	0.341	0.277	0.391	0.621	0.588
1.0	0.245	0.33	0.346	0.352	0.573	0.627
0.8	0.263	0.317	0.205	0.324	0.485	0.496
0.4	0.236	0.311	0.317	0.314	0.508	0617
0.2	0.265	0.271	0.022	0.398	0.496	0.242
0.0	0.239	0.259	0.083	0.341	0.491	0.439

From the above table, the yeast cellular growth analyzed under anaerobic conditions differs distinctly from that of aerobic growth pattern. Initially, the control group in the anaerobic conditions have a lower growth rate with an end point cell number of 0.287 cells/ml as compared with 0.315 cells/ml at calcitriol treated group. On the contrary under aerobic conditions, the cell density end point was measured as 0.428 cells/ml and 0.724 cells/ml with control and calcitriol treated group respectively.

The calculated difference between calcitriol and control groups are tabulated in (B-A)/A column. By comparing these values in aerobic and anaerobic conditions, we could deduce a significant difference occurring in the cell density end points at both conditions. However, at lower calcium concentration range (0.0 µg/ml), both of their cell numbers looks similar ranging from 0.239 to 0.259 cells/ml in anaerobic conditions and 0.341 and 0.491cells/ml at aerobic conditions. This indicates the tolerance levels of cells towards calcitriol signaling mechanism under lower calcium concentrations. The results verify that the yeast system maintains a calcitriol therapeutic action under anaerobic conditions, however, its therapeutic effect is reduced considerably compared to aerobic conditions. This observation is a novel contribution produced by our model, which provides insights that most of the free calcium molecule are transported along with oxygen elements in the human bloodstream (or) cytosolic space in the yeast system because of the high oxygen affinity possessed by the calcitriol. During its transport in the bloodstream, higher binding of non-metabolized calcitriol occurs with oxygen elements that might lead to its hypercalcemic effects.

5.7.1 Anaerobic Intracellular Calcium

To further test this hypothesis, we detected the intracellular calcium levels occurring under anaerobic conditions using fluorescent detection technique. The study was repeated as provided in the aerobic conditions. However, the cell number was normalized to match the aerobic cell count of 10^9 cells /ml. The final fluorescent results are listed in table 19 and the data has been plotted in figure 17.

Table 19 Anaerobic Intracellular calcium levels

The table displays the intracellular calcium levels on calcitriol treated and control cells imaged under anaerobic conditions.

Calcium Concentration Range (M)	Calcitriol Imaged Cells (mM Ca^{2+})	Control Imaged cells (mM Ca^{2+})
0.5M	2.26	2.31
0.25M	2.04	2.12
0.125M	1.87	2.06
0.0625M	1.79	1.98
0.0312M	1.24	1.31
0.0156M	1.09	1.189
0.0078M	0.874	0.9

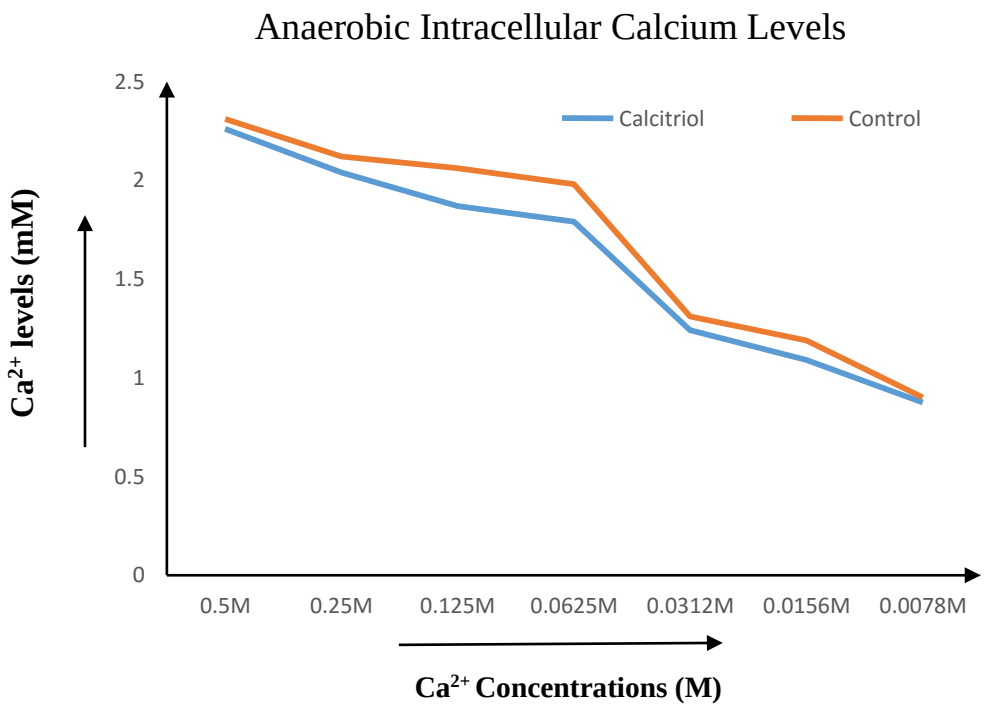

Figure 17 Intracellular calcium levels under Anaerobic Conditions

The graph in figure 17 illustrates a considerable range of similarity occurring in the intracellular calcium levels of both the calcitriol and control treated group under anaerobic conditions.

The table 19 provides the cellular calcium levels that are imaged under the Ca^{2+} concentration range; 0.5M, 0.25M, 0.125M, 0.0625M, 0.0312M, 0.0156M, 0.0078M. The corresponding intracellular calcium levels obtained under these Ca^{2+} concentrations in calcitriol treated cells are 2.26, 2.04, 1.87, 1.79 1.24, 1.09, 0.874. Similarly, the control treated group showed 2.31, 2.12, 2.06, 1.98, 1.31 1.189 and 0.9 calcium levels respectively. As seen from the results tabulated above, the calcitriol imaged cells at these calcium concentrations shows similar calcium levels in comparison with that of control imaged cells. These values are depicted in the graph in figure 17, in which the orange curve denotes the calcium ion transportation in control cells whereas the blue curve represents the calcitriol treated cells. The Ca^{2+} ion transportation in both the groups overlaps each other, which highlights the stability of Ca^{2+} ion concentration towards calcitriol under anaerobic conditions. As we propose, oxygen affinity plays a key role in calcitriol functionality. Figure 17 provides a suitable explanation for the hypercalcemic effects occurring due to the oxygen affinity of calcitriol. Moreover, we can conclude that optimal conditions of oxygen levels and calcium concentration together activate the calcitriol functionality to perform as a cell protective agent or a toxic agent to kill abnormal cells.

5.7.2 Aspartate Glutamate Shock Analysis

The second hypothesis in the same yeast system is the amino-acid shock analysis that we proposed based upon the EF binding motif. Here we analyzed the active role of two main amino acids: Aspartate and Glutamate that might contribute to the calcium signaling effects of calcitriol. In this experiment, yeast system is systemically stressed by preparing a synthetic medium that contains an excess of these two amino-acids. This might show that both oxygen affinity and aspartate-glutamate amino acids are inversely related to each other causing changes in the performance of the drug. In this procedure, we analyzed normal yeast cells and also a highly inhibited mutant strain MID1/YNL291C is exposed to the amino acid excess conditions at optimal calcium concentration. The results are plotted as graphs in figure 18. The curve (a) in figure 18 depicts the calcitriol treatment with the normal cells. During the treatment of normal cells, the calcitriol treated group and control group together reaches an OD of 2.0 at the end of 24 hour period. However, there is a fluctuation pattern during their normal growth, which could be neglected. On the other end, in a gene deletion strain represented in curve (b), there is a clear inhibition occurring in calcitriol treated group from that of a control group with an OD difference between1.6 to 1.8.

It formalizes that the calcitriol reactivity is being neutralized in the case of normal cells and its activity is being reduced in the case of gene deletion cells due to the stress created from the two excess amino acids. However, calcitriol still inhibits the abnormal mutant strain, but when compared with the high toxic effect produced under optimal conditions before, the therapeutic activity of the drug towards this genomic strain is vastly reduced under these amino-acid stress conditions.

- Normal-Calcitriol

(a)

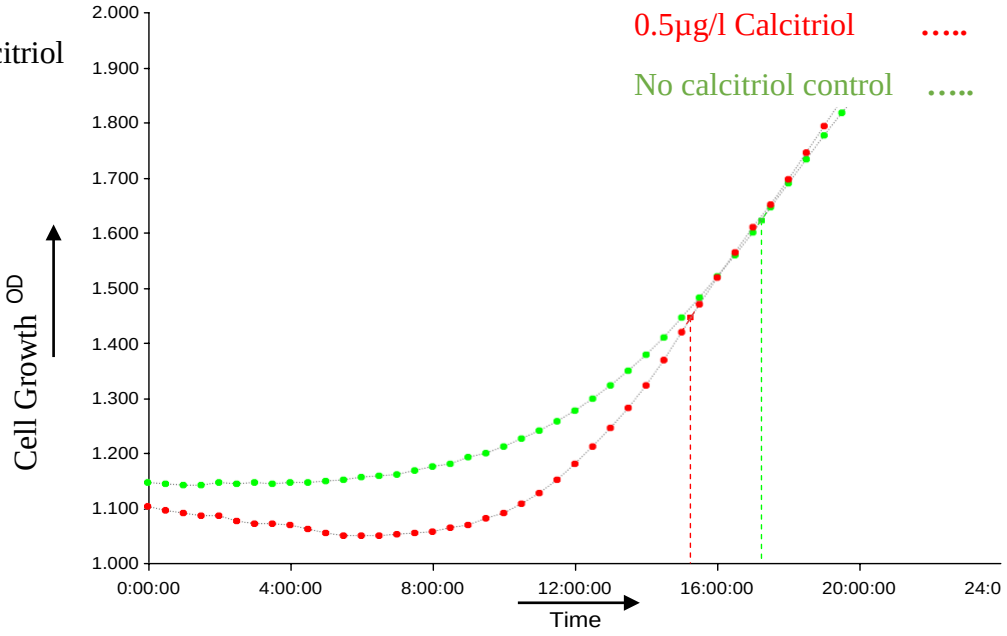

- Mutant-Calcitriol

(b)

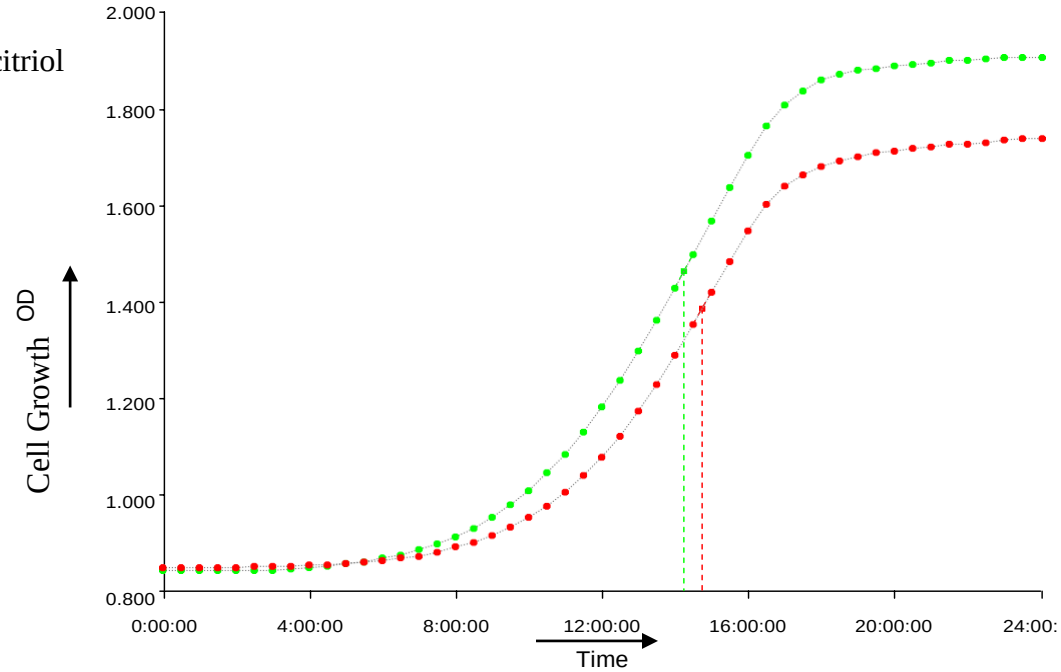

Figure 18 Growth Rate Analysis under Aspartate-Glutamate Stress conditions.

The figure 18(a) and 18(b) depict the calcitriol and control activity on normal yeast cells and on a selected genomic strain (MID1). Both of them perform under aspartate- glutamate stress conditions.

5.8 Oxidative Stress analysis for Free radical Generation

The results for the oxidative stress analysis conducted under UV-A exposure and AAPH are displayed in tables 20 and 21.

Table 20 UV-A Cell Irradiation

Cell Number(cells/ml)	Time interval (Hour)	Calcitriol Cell density end point (cells/ml)	Control Cell density end point (cells/ml)
$1.5x\ 10^7$	2	1.682	1.675
$1.5x\ 10^7$	4	1.514	1.521
$1.5x\ 10^7$	6	1.328	1.319
$1.5x\ 10^7$	8	1.297	1.216
$1.5x\ 10^7$	10	1.264	1.253

Table 21 AAPH Treatment

Cell Number(cells/ml)	Time interval (Hour)	Calcitriol cell density end point (cells/ml)	Control Cell density end point(cells/ml)
$1.5x\ 10^7$	2	1.052	1.021
$1.5x\ 10^7$	4	0.986	0.431
$1.5x\ 10^7$	6	0.654	0.229
$1.5x\ 10^7$	8	0.453	0.103
$1.5x\ 10^7$	10	0.321	0.002

In table 20, the calcitriol and control cell concentration end points were measured for a period of 10 hours with a 2 hour interval period. Their cell number differed negligibly ranging from 1.682-1.264 in calcitriol treated group during the ten hour period. When control cells are exposed to UV-A irradiation, they displayed similar cellular reactivity with their cell number ranging from 1.675 to 1.253. This shows that UV-A doesn't have much effect towards the growth of cells. This irradiating effect caused only minimal changes in stressing the yeast cells which can be seen from the overall cell density. From this understanding, we can't verify the anti-oxidant property of calcitriol.

In order to understand this anti-oxidative theory of calcitriol, we proposed the use of AAPH which is clearly shown to have generated free radicals at a continuous pace when used to treat viable cells. The results from AAPH treatment are tabulated in table 21. The table provides the list of calcitriol treated and control cell density end points over a 10 hour period. The calcitriol cell density end point during this 10 hour period undergoes an elusive amount of death with their cell number declining from 1.052 to 0.321 cells/ml. On the other hand, the control cell density end point also produces excessive death number with their cell count ranging from 1.021 to 0.002 cells/ml. From this analysis, we can conclude that the growth is diminished almost completely over a 10 hour period during AAPH treatment, but when compared with the control, the calcitriol treated cells displayed a higher cell growth order which possibly might provide a support for the anti-oxidative mechanisms of calcitriol.

5.9 Yeast Aging Model

To further test the anti-oxidative theory of calcitriol, we developed a yeast aging model by studying its growth rate over a period of 21 days. The results for this yeast aging model are listed in table 22 and the graph for the corresponding data are displayed in figure 19.

Table 22 Yeast Aging Study

S. No	Time interval (days)	Calcitriol incubated cell group (cells/ml)	Control cell group (cells/ml)
1	2	2.533	2.219
2	5	2.198	1.986
3	8	2.076	1.754
4	12	1.893	1.479
5	15	1.388	1.109
6	18	1.162	0.789
7	21	0.876	0.421

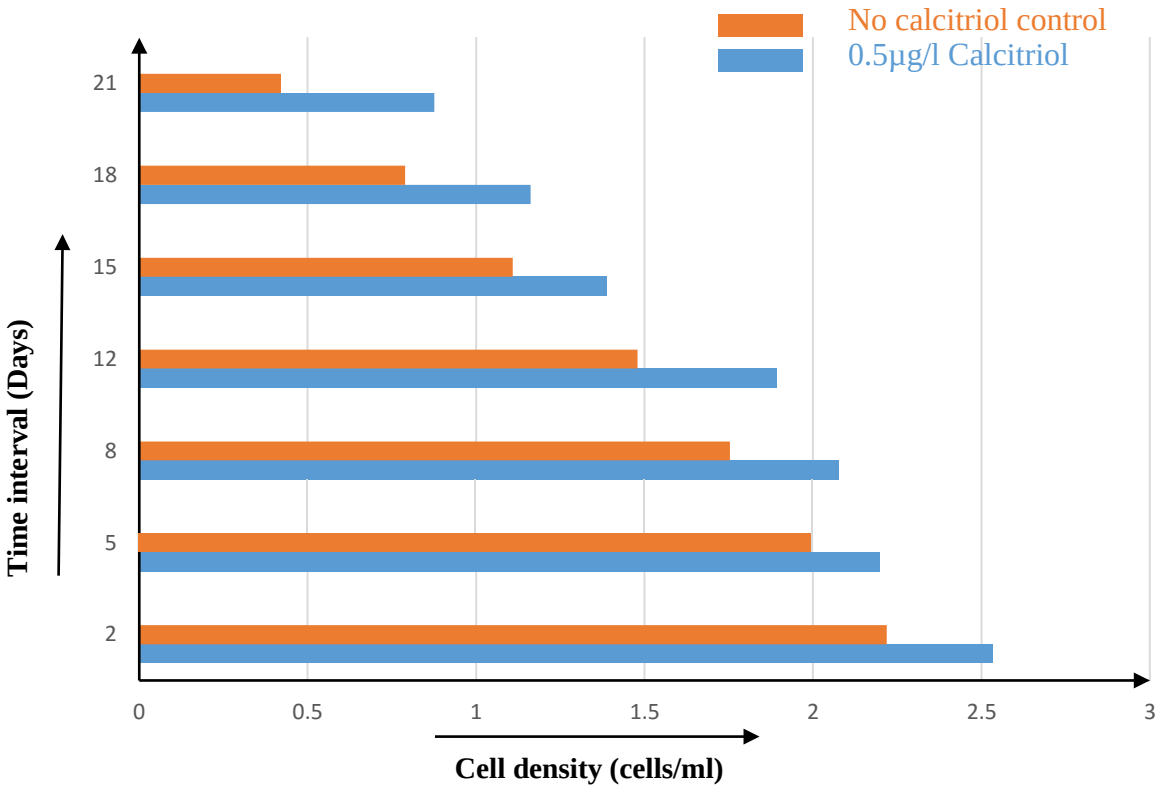

Figure 19 Yeast Aging Study

The bar chart represents the calcitriol effect on yeast cells at seven different age points

From table 22, the cellular density end point at 2 day period in calcitriol treated group records 2.533 cells/ml and in control cell group, it is 2.219 cells/ml. On further study with varying time intervals, the aging interval points are noted at the end of 5, 8, 12, 15, 18, and 21. During the course of this analysis, the cell number in calcitriol treated group is seemingly high as compared to that of a control group. At the final end of 21 day study period, the calcitriol treated group showed a cell density end point of 0.876 cells/ml and the control treated group showed a cell density end point of 0.421 cells/ml. The data is represented in the form of a bar chart in figure 19. The blue line represents the calcitriol treated group and the orange line depicts the control group. In this procedure, the calcitriol treated group demonstrated an enhanced growth of cells counteracting the aging process whereas the control group underwent cell deterioration at a faster pace. This analysis provides an impact on cell-aging mechanisms of calcitriol to prevent the cell from undergoing any kind of cell damage. From this study, we set a landmark for using calcitriol as an effective anti-aging compound in a cellular level.

5.10 Model limitations

This work was particularly focused on calcemic effects associated with the drug in the cellular activities. Even if this work provides an overview on the calcium signaling effects of calcitriol towards the yeast system, the real human model has complicated mechanisms involving blood circulation, intestinal calcium absorption and the elimination activities occurring via kidneys. The proposed model has the ability to determine the calcitriol functionality by integrating all cellular functionality into one yeast system. However, it suffers from a weak modelling that could not be prototyped for multicellular organisms and therefore, cannot be used as an efficient resource for clinical applications/medical purposes.

The current results were built based on selected genome functions, which can be considered as a calcium transport channeling approximation. Still higher order genomic analysis involving drug profiling over a complete set of gene deletion strains is needed which could contribute to greater insights on the chemical genetic interactions of calcitriol. However, since we used calcitriol, which is a highly calcium oriented targeting drug when administered/treated into the system, can trigger one step activation of these analyzed calcium channels and thus it can be accurately modelled for its calcemic effects in a yeast system.

5.11 Conclusion

In this chapter, we discussed the results obtained from the drug with the proposed yeast model system. It is a real model pharmacokinetic analysis conducted based on calcium concentration parameter and cellular drug metabolisms.

Chapter 6. Conclusion and future work

6.1 Summary of work

In this project, we were motivated to develop a model to investigate the effects of a Vitamin D metabolite called calcitriol. Calcitriol is an active metabolite that is predominantly synthesized in the human skin naturally from sunlight at UVB wavelength of 295-320 nm. It is the only natural vitamin drug that has been approved for treating epileptic patients and neural disorders. It is also used in conjugated chemotherapy during cancer treatments because of the benefit it provides in the natural targeting of the drug at the target site of tissue. Despite these uses, there are issues related to its hypercalcemic effects in treated patients and the relative cost associated with the production of synthetic calcitriol analogs. Chemotherapeutic agents conjugated with calcitriol has the feature of a localizing target molecule to a specific receptor in the body. The main contribution of this work was to propose a yeast system model to study the mechanisms of calcitriol in cellular functions to overcome the above-mentioned limitations. Hence, we developed and simulated the yeast system with calcitriol binding mechanism based on computational approach supported by experimental data.

Pharmacokinetic drug profiling in yeast system is a simplistic approach to deal with targeted therapeutic mechanisms and for that, we studied the physiological concentration parameters related to calcium signaling mediated by calcitriol. We developed an approach to determine the toxicity/protective effects of calcitriol in the yeast system which is used to further propose a more advanced theory. We used fluorescent imaging and an anaerobic model to infer that calcium ion transportation is controlled by the oxygen affinity in the blood circulation/cytosolic space.

The cellular calcium concentration in each compartment (depending on the site of drug action) is independent of calcitriol therapeutic action however we could claim that in humans, based upon the hemoglobin which carries the oxygen molecule, that might control these calcemic effects caused by calcitriol due to its oxygen affinity leading to the elevation of serum calcium levels in the blood serum.

6.2 Future work

Due to the complicated mechanisms associated with the human model and also in the absence of real data obtained from clinical practices, the data developed from the proposed work can serve just as a first stage model. The next stage of this work would be to implement a recombinant approach to clone human VDR into the yeast genome and investigate its behavior when exposed to calcitriol at different calcium concentrations. Also, all the yeast deletion strains should be studied and precisely evaluated to understand the complete genomic regulation associated with calcitriol signaling networks. Indeed, it is essential to re-evaluate the drug dosage and parameters based on other ion concentration parameters such as Magnesium /PTH regulation and to determine the calcitriol-mediated hypercalcemic effects, which we assume from our analysis to be associated with oxygen parameter. Therefore, we must work in an anaerobic work station chamber and optimize the oxygen concentrations relating to the calcitriol treatment. By optimizing the oxygen parameter as we did with the calcium parameter, we might be able to validate our hypothesis. It is, therefore, crucial to evaluate such key parameters in our study. Finally, we should evaluate the therapeutic IC50 concentration for calcitriol in mammalian cells which is suitable for the drug to target the specific site of a receptor at 50% absorption rate.

APPENDICES

A.1 Materials Required

Rocaltrol (Calcitriol 0.5mcg) has been purchased from pharmacy. AAPH (2, 2'-Azobis (2-amidinopropane) dihydrochloride) (Product Id: 440914 Aldrich) and Indo -1 Pentapossium salt (Catalog number: I-1202) were purchased from Sigma Aldrich Ltd and ThermoFisher Scientific Ltd, respectively.

A.2 Buffer preparation for Fluorescent Cell Imaging

Loading Buffer

- 10mM MES (2-(N-morpholino) ethanesulfonic acid)
- 50mM KCl
- 20mm Indo-1 pentapotassium dye
- pH is maintained at 4.5

Washing Buffer

- 10mM MES
- 0.1Mm EDTA
- 0% dye
- pH is maintained at 4

Ca-EGTA Buffer

- 170mM KCl; 35mM Nacl; 25mM Mgcl2
- 10mM MES/Tris Buffer
- 0.1µm Indo-1 Pentapotassium dye
- pH is maintained at 6.2
- R min measured after the addition of 10N NaOH and 1mM EGTA with a pH value maintained at 8 without any calcium addition.
- R max measured after the addition of known concentrations of $CaCl_2$

A.3 Calcium Stress Conditions

Table 23 Calcium Stress Analysis: Media Preparation [74]

Ca2+ Normal Yeast system	Ca2+ Deficient Yeast system	Ca2+ Excessive Yeast system	Glucose Deficient Yeast system
1% Bactoyeast	0.67% Bactoyeast	2% Bactoyeast	0.67% Bactoyeast
2% Bactopeptone	2% Dextrose	4% Bactopeptone	0.001% Dextrose
2% Dextrose		2% Dextrose	

Table 24 Plate set up for drug concentration profiling

	1	2	3	4	5	6	7	8	9
A	**170NM 30C 50CC 0G**	**150NM 30C 50CC 20G**	**130NM 30C 50CC 40G**	**110NM 30C 50CC 60G**	**90NM 30C 50CC 80G**	**70NM 30C 50CC 100G**	**50NM 30C 50CC 120G**	**30NM 30C 50CC 140G**	**10NM 30C 50CC 160G**
	1.6Ca2+	***1.4Ca2+***	***1.2Ca2+***	***1.0Ca2+***	***0.8Ca2+***	***0.6Ca2+***	***0.4Ca2+***	***0.2Ca2+***	***0.0Ca2+***
B	**170NM 30W 50CC 0G**	**150NM 30W 50CC 20G**	**130NM 30W 50CC 40G**	**110NM 30W 50CC 60G**	**90NM 30W 50CC 80G**	**70NM 30W 50CC 100G**	**50NM 30W 50CC 120G**	**30NM 30W 50CC 140G**	**10NM 30W 50CC 160G**
C	**250NM**	**250NM**	**250NM**	**250NM**	**250NM**	**250NM**	**250NM**	**250NM**	**250NM**
D									
E									
F	**170EM 30C 50CC 0G**	**150EM 30C 50CC 20G**	**130EM 30C 50CC 40G**	**110EM 30C 50CC 60G**	**90EM 30C 50CC 80G**	**70EM 30C 50CC 100G**	**50EM 30C 50CC 120G**	**30EM 30C 50CC 140G**	**10EM 30C 50CC 160G**
	3.2Ca2+	***3.0Ca2+***	***2.8Ca2+***	***2.6Ca2+***	***2.4Ca2+***	***2.2Ca2+***	***2.0Ca2+***	***1.8Ca2+***	***1.6Ca2+***
G	**170EM 30W 50CC 0G**	**150EM 30W 50CC 20G**	**130EM 30W 50CC 40G**	**110EM 30W 50CC 60G**	**90EM 30W 50CC 80G**	**70EM 30W 50CC 100G**	**50EM 30W 50CC 120G**	**30EM 30W 50CC 140G**	**10EM 30W 50CC 160G**
H	**250EM**	**250EM**	**250EM**	**250EM**	**250EM**	**250EM**	**250EM**	**250EM**	**250EM**

NM- Normal Media ; EM- Excessive Media

C-Calcitriol; CC- Cell Culture; W- Water; G- Glucose

A.3 Glucose Concentration Preparation

Table 25 Drug Optimal Concentration Plate Set up

	1	2	3	4	5	6	7
A	**170NM 30C 50CC 0G**	**160NM 30C 50CC 10G**	**150NM 30C 50CC 20G**	**140NM 30C 50CC 30G**	**130NM 30C 50CC 40G**	**120NM 30C 50CC 50G**	**110NM 30C 50CC 60G**
	1.6Ca2+	***1.5Ca2+***	***1.4Ca2+***	***1.3Ca2+***	***1.2Ca2+***	***1.1Ca2+***	***1.0Ca2+***
B	**170NM 30W 50CC 0G**	**160NM 30W 50CC 10G**	**150NM 30W 50CC 20G**	**140NM 30W 50CC 30G**	**130NM 30W 50CC 40G**	**120NM 30W 50CC 50G**	**110NM 30W 50CC 60G**
C	**250NM**	**250NM**	**250NM**	**250NM**	**250NM**	**250NM**	**250NM**

NM – Normal Media; C – Calcitriol; CC – Cell Culture

G - Glucose; W - Water

A.4 Aging Media

Table 26 Yeast Aging Study

Component	Concentration (g/L)
D-glucose	20
Yeast nitrogen base (-AA/AS)	1.7
(NH4)2SO4	5.0
Adenine	0.04
L-Arginine	0.02
L-Aspartic acid	0.1
L-Glutamic acid	0.1
L-Histidine	0.1
L-Leucine	0.3
L-Lysine	0.03
L-Methionine	0.02
L-Phenylalanine	0.05
L-Serine	0.375
L-Threonine	0.2
L-Tryptophan	0.04
L-Tyrosine	0.03
L-Valine	0.15
Uracil	0.1

References

[1] Holick, M. (2007). Vitamin D Deficiency, New England Journal of Medicine, Vol. 357, No. 3, pp. 266-281.

[2] Harms, L., Burne, T., Eyles, D., and McGrath, J. (2011). Vitamin D and the brain, Best Practice & Research Clinical Endocrinology & Metabolism, Vol. 25, No. 4, pp. 657-669.

[3] Thandrayen, K., and Pettifor, J. (2010). Maternal Vitamin D Status: Implications for the Development of Infantile Nutritional Rickets. Endocrinology and Metabolism Clinics of North America, Vol. 39, No. 2, pp. 303-320.

[4] Norris, N. (2001). Can the sunshine vitamin shed light on type 1 diabetes? The Lancet, Vol. 358, No. 9292, pp. 1476-1478.

[5] Scorza, F., Albuquerque, M., Arida R., Terra, V., Machado, H., and Cavalheiro, E. (2010). Benefits of sunlight: Vitamin D deficiency might increase the risk of sudden unexpected death in epilepsy. Medical Hypotheses, Vol. 74, No. 1, pp. 158-161.

[6] Shellhaas, R., and Joshi, S. (2010). Vitamin D and Bone Health among Children with Epilepsy. Pediatric Neurology, Vol. 42, No. 6, pp. 385-393.

[7] Herrling, T. (2003). UV-induced free radicals in the skin detected by ESR spectroscopy and imaging using nitroxides. Free Radical Biology and Medicine, Vol. 35, No. 1, pp. 59-67.

[8] Trump, D., Hershberger, P., Bernardi, R., Ahmed, S., Muindi, J., Fakih, M., Yu, W., and Johnson, C. (2004). Anti-tumor activity of calcitriol: pre-clinical and clinical studies. The Journal of Steroid Biochemistry and Molecular Biology, Vol. 89-90, pp. 519-526.

[9] Botstein, D. (1997). Genetics: Yeast as a Model Organism. Science, Vol. 277, No. 5330, pp. 1259-1260.

[10] Norval, M., Björn, L., and Gruijl, F. (2010). Is the action spectrum for the UV-induced Production of previtamin D 3 in human skin correct? Photochemical & Photobiological Sciences, Vol. 9, No. 1, pp. 11-17.

[11] Andress, D., Norris, K., Coburn, J., Slatopolsky, E., and Sherrard, D. (1989). Intravenous Calcitriol in the Treatment of Refractory Osteitis Fibrosa of Chronic Renal Failure. New England Journal of Medicine, Vol. 321, No. 5, pp. 274-279.

[12] Grace, K. (2010). The Rationale behind Topical Vitamin D Analogs in the Treatment of Psoriasis Where Does Topical Calcitriol Fit In? The Journal of Clinical and Aesthetic Dermatology, Vol. 382010, No. 2945865.

[13] Lips, P. (2001). Vitamin D Deficiency and Secondary Hyperparathyroidism in the Elderly: Consequences for Bone Loss and Fractures and Therapeutic Implications. Endocrine Reviews, Vol. 22, No. 4, pp. 477-501.

[14] Krishnan, A., Swami, S., and Feldman, D. (2010). Vitamin D and breast cancer: Inhibition of estrogen synthesis and signaling. The Journal of Steroid Biochemistry and Molecular Biology, Vol. 121, No. 1-2, pp. 343-348.

[15] Fraga, R., Zacconi, F., Sussman, F. (2011). 'Design, Synthesis, Evaluation, and Structure of Vitamin D Analogues with Furan Side Chains', Chemistry - A European Journal, vol. 18, No. 2, pp. 603-612.

[16] Norman, A., Bishop, J., Bula, C., Olivera, C., Mizwicki, M., Zanello, L., Ishida, H., and Okamura, W. (2002). Molecular tools for study of genomic and rapid signal transduction responses initiated by 1α, 25 (OH) 2-vitamin D 3. Steroids, Vol. 67, No. 6, pp. 457-466.

[17] Narayanan, D. L., Saladi, R., and Fox, J. (2010). Review: 'Ultraviolet radiation and skin cancer'. International Journal of Dermatology, Vol. 49, No. 9, pp. 978-986.

[18] Quinn, C. (2010). Vitamin D: the sunshine vitamin. British Journal of Nursing, Vol. 19, No. 18, pp. 1160-1163.

[19] Falcao Pedrosa Costa, A., Machado dos Reis, L., Custodio Ribeiro, M., Maria Affonso Moyses, R., and Jorgetti, V. (2003). Effects of calcitriol on parathyroid function and on bone remodelling in secondary hyperparathyroidism. Nephrology Dialysis Transplantation, Vol. 18, No. 4, pp. 743-749.

[20] Chun, R. (2012). New perspectives on the vitamin D binding protein. Cell Biochemistry and Function, Vol. 30, No. 6, pp. 445-456.

[21] Trump, D., and Johnson, C. (2011). Vitamin D and cancer. New York: Springer.

[22] Masaki, H., Atsumi, T., and Sakurai, H. (1995). Detection of Hydrogen Peroxide and Hydroxyl Radicals in Murine Skin Fibroblasts under UVB Irradiation. Biochemical and Biophysical Research Communications, Vol. 206, No. 2, pp. 474-479.

[23] Koutkia, P., Lu, Z., Chen, T., and Holick, M. (2001). Treatment of vitamin D deficiency due to Crohn's disease with tanning bed ultraviolet B radiation. Gastroenterology, Vol. 121, No. 6, pp. 1485-1488.

[24] Holick, M. (2009). Vitamin D Status: Measurement, Interpretation, and Clinical Application. Annals of Epidemiology, Vol. 19, No. 2, pp. 73-78.

[25] Matsushima, N., Tokita, M., and Hikichi, K. (1986). X-ray determination of the crystallinity in bone mineral. Biochimica ET Biophysica Acta, Vol. 883, No. 3, pp. 574-579.

[26] Loong, C., Rey, C., Kuhn, L., Combes, C., Wu, Y., Chen, S., and Glimcher, M. (2000). Evidence of hydroxyl-ion deficiency in bone apatites: an inelastic neutron-scattering study. Bone, Vol. 26, No. 6, pp. 599-602.

[27] Fernández-Seara, M., Wehrli, S., Takahashi, M., and Wehrli, F. (2003). Water Content Measured by Proton-Deuteron Exchange NMR Predicts Bone Mineral Density and Mechanical Properties. Journal of Bone and Mineral Research, Vol. 19, No. 2, pp. 289-296.

[28] Kai, A., and Miki, T. (1989). Electron Spin Resonance of Organic Radicals Derived from Amino Acids in Calcified Fossils. Japanese Journal of Applied Physics, Vol. 28, No. 11, pp. 2277-2282.

[29] Schäferling, M. (2012). The Art of Fluorescence Imaging with Chemical Sensors. Angewandte Chemie International Edition, Vol. 51, No. 15, pp. 3532-3554.

[30] Mitschele, J. (1996). Beer-Lambert Law. Journal of Chemical Education, Vol. 73, No. 11, pp. 1007-1099.

[31] Bio-rad.com, 'Detection Methods | Applications & Technologies | Bio-Rad', 2015. [Online]. Available:http://www.bio-rad.com/en-hr/applications-technologies/detection-methods. [Last Accessed: 05- Nov- 2015].

[32] Halachmi, D., and Eilam, Y. (1989). Cytosolic and vacuolar Ca2+ concentrations in yeast cells measured with the Ca2+-sensitive fluorescence dye indo-1. Federation of European Biochemical Societies FEBS Letters, Vol. 256, No. 1-2, pp. 55-61.

[33] Spencer, J., and Amonette, R. (1995). Indoor tanning: Risks, benefits, and future trends. Journal of the American Academy of Dermatology, Vol. 33, No. 2, pp. 288-298.

[34] Zamboni, M., and Zoico, E. (2000). Vitamin D, physical performance and disability in the elderly. Aging Clinical and Experimental Research, Vol. 12, No. 6, pp. 405-406.

[35] Wiseman, H. (1993). Vitamin D is a membrane antioxidant Ability to inhibit iron- dependent lipid peroxidation in liposomes compared to cholesterol, ergosterol and tamoxifen and relevance to anticancer action. Federation of European Biochemical Societies FEBS Letters, Vol. 326, No. 1-3, pp. 285-288.

[36] MacLaughlin, J., Anderson, R., and Holick, M. (1982). Spectral character of sunlight modulates photosynthesis of previtamin D3 and its photoisomers in human skin. Science, Vol. 216, No. 4549, pp. 1001-1003.

[37] Bouillon, R., et al. (2006). Action spectrum for production of previtamin D3 in human skin. Technical Report 174, Commission Internationale de l'Éclairage (CIE), Central Bureau, Vienna, Austria.

[38] Morrow, C. (2007). Cholecalciferol poisoning. Veterinary Medicine, Vol. 96, No.12, pp. 905-911.

[39] Rostand, D., and Drueke, T. (1999). Parathyroid hormone, vitamin D, and cardiovascular disease in chronic renal failure. Kidney International, Vol. 56, No. 2, pp. 383-392.

[40] Pubchem, 'calcitriol | C27H44O3 - PubChem', 2015. [Online]. Available: http://pubchem.ncbi.nlm.nih.gov/compound/calcitriol. [Last Accessed: 05- Nov- 2015].

[41] Armstrong, B., and Kricker, A. (2001). The epidemiology of UV induced skin cancer. Journal of Photochemistry and Photobiology B: Biology, Vol. 63, No. 1-3, pp. 8-18.

[42] Summerday, N. et al. (2007). Vitamin D and Multiple Sclerosis: Review of a Possible Association. Journal of Pharmacy Practice, Vol. 25, No. 1, pp. 75-84).

[43] Hirata, M., Endo, K., Katsumata, K., Ichikawa, F., Kubodera, N., and Fukagawa, M. (2002). A comparison between 1, 25-dihydroxy-22-oxavitamin D3 and 1, 25-dihydroxyvitamin D3 regarding suppression of parathyroid hormone secretion and calcaemic action. Nephrology Dialysis Transplantation, Vol. 17, No. 10, pp. 41-45.

[44] Espinosa, P., Perez, D., Abner, E., and Ryan, M. (2011). Association of antiepileptic drugs, vitamin D, and calcium supplementation with bone fracture occurrence in epilepsy patients. Clinical Neurology and Neurosurgery, Vol. 113, No. 7, pp. 548-551.

[45] Jones, G. (2012). Vitamin D Analogs. Rheumatic Disease Clinics of North America, Vol. 38, No. 1, pp. 207-232.

[46] Bikle, D. (2009). Nonclassic Actions of Vitamin D. The Journal of Clinical Endocrinology & Metabolism, Vol. 94, No. 1, pp. 26-34.

[47] Boekhout, T. (2003). Yeasts in food. Cambridge: Woodhead Publishing Ltd.

[48] Cui, J et al. (2009). Calcium homeostasis and signaling in yeast cells and cardiac myocytes. FEMS Yeast Research, Vol. 9, No. 8, pp. 1137-1147.

[49] Cui, J., and Kaandorp, J. (2006). Mathematical modeling of calcium homeostasis in yeast cells. Cell Calcium, Vol. 39, No. 4, pp. 337-348.

[50] Peppas, N. (1996). Receptors: models for binding, trafficking, and signaling. Journal of Controlled Release, Vol. 39, No. 1, pp. 105-106.

[51] Tovchigrechko, A., Wells, C., and Vakser, I. (2002). Docking of protein models. Protein Science, Vol. 11, No. 8, pp. 1888-1896.

[52] Berman, H. (2000). The Protein Data Bank. Nucleic Acids Research, Vol. 28, No. 1, pp. 235-242).

[53] Makarewicz, T., and Kaźmierkiewicz, R. (2013). Molecular Dynamics Simulation by GROMACS Using GUI Plugin for PyMOL. Journal of Chemical Information and Modeling, Vol. 53, No. 5, pp. 1229-1234.

[54] Hsu, K., Chen, Y., Lin, S., and Yang, J. (2011). iGEMDOCK: a graphical environment of enhancing GEMDOCK using pharmacological interactions and post-screening analysis. BMC Bioinformatics, Vol. 12, No. 1, pp. 1-33.

[55] Rice, P., Longden, I., and Bleasby, A. (2000). EMBOSS: The European Molecular Biology Open Software Suite. Trends in Genetics, Vol. 16, No. 6, pp. 276-277.

[56] Rodríguez-Tudela, J et al. (2003). Method for the determination of minimum inhibitory concentration (MIC) by broth dilution of fermentative yeasts. Clinical Microbiology and Infection, Vol. 9, No. 8, pp. i-viii.

[57] Denis, V. (2002). Internal Ca^{2+} release in yeast is triggered by hypertonic shock and mediated by a TRP channel homologue. The Journal of Cell Biology, Vol. 156, No. 1, pp. 29-34.

[58] Shinpo, K., Kikuchi, S., Sasaki, H., Moriwaka, F., and Tashiro, K. (2000). Effect of 1, 25-dihydroxyvitamin D3 on cultured mesencephalic dopaminergic neurons to the combined toxicity caused by L-buthionine sulfoximine and 1-methyl-4-phenylpyridine. Journal of Neuroscience Research, Vol. 62, No. 3, pp. 374-382.

[59] Puttaiah, R., Griggs, J., and D'Onofrio, M. (2014). A Preliminary Evaluation of a Reusable Digital Sterilization Indicator Prototype. The Journal of Contemporary Dental Practice, Vol. 15, No. 5, pp. 626-635.

[60] Altschul, S., Gish, W., Miller, W., Myers, E., and Lipman, D. (1990). Basic local alignment search tool. Journal of Molecular Biology, Vol. 215, No. 3, pp. 403-410.

[61] Wasserman, R. (1969). Binding Proteins from Animals with Possible Transport Function. The Journal of General Physiology, Vol. 54, No. 1, pp. 114-137.

[62] Piszczatowski, R et al. (2014). The glyceraldehyde 3-phosphate dehydrogenase gene (GAPDH) is regulated by myeloid zinc finger 1 (MZF-1) and is induced by calcitriol. Biochemical and Biophysical Research Communications, Vol. 451, No. 1, pp. 137-141.

[63] Dong, J et al. (2012). Calcitriol protects renovascular function in hypertension by down-regulating angiotensin II type 1 receptors and reducing oxidative stress. European Heart Journal, Vol. 33, No. 23, pp. 2980-2990.

[64] Cavalier, E et al. (2011). Vitamin D and type 2 diabetes mellitus: Where do we stand? Diabetes & Metabolism, Vol. 37, No. 4, pp. 265-272.

[65] Dröge, W. (2002). Free Radicals in the Physiological Control of Cell Function. Physiology Reviews, Vol. 82, No. 1, pp. 47-95.

[66] Zou, C., Agar, N., and Jones, G. (2001). Oxidative insult to human red blood cells induced by free radical initiator AAPH and its inhibition by a commercial antioxidant mixture. Life Sciences, Vol. 69, No. 1, pp. 75-86.

[67] Vile, G., and Tyrrell, R. (1995). UV-A radiation-induced oxidative damage to lipids and proteins in vitro and in human skin fibroblasts is dependent on iron and singlet oxygen. Free Radical Biology and Medicine, Vol. 18, No. 4, pp. 721-730.

[68] Coelho, S., and Hearing, V. (2009). UVA tanning is involved in the increased incidence of skin cancers in fair-skinned young women. Pigment Cell & Melanoma Research, Vol. 23, No. 1, pp. 57-63.

[69] Murakami, C., and Kaeberlein, M. (2009). Quantifying Yeast Chronological Life Span by Outgrowth of Aged Cells. Journal of Visualized Experiments, No. 27, 1176, pp. 1-5.

[70] Liu, W. 2012. Introduction to modeling biological cellular control systems. Milan: Springer.

[71] Grynkiewicz et al. (1985). A new generation of Ca2+ indicators with greatly improved Fluorescence Properties. Journal of Biological Chemistry, Vol. 260, No. 6, pp.3440-3450.

[72] Darvishi, E., Omidi, M., Bushehri, A., Golshani, A and Smith, M. (2013). The Antifungal Eugenol Perturbs Dual Aromatic and Branched-Chain Amino Acid Permeases in the Cytoplasmic Membrane of Yeast. PLOS ONE, Vol. 8, No. 10, e76028.

[73] Biotek.com, 'Gen5 Data Analysis Software', 2015. [Online]. Available: http://www.biotek.com/products/product_print.html?newsid=149. [Last Accessed: 11- Nov- 2015].

[74] BD, 'BD Bio nutrients - Technical Manual Advanced Bioprocessing', 2015. [Online]. Available: https://www.bd.com/ds/technicalCenter/misc/br_3_2547.pdf. [Last Accessed: 05- Nov- 2015].